

NASA Technical Memorandum 108481

Statistically Generated Weighted Curve Fit of Residual Functions for Modal Analysis of Structures

*P.S. Bookout
Marshall Space Flight Center • MSFC, Alabama*

National Aeronautics and Space Administration
Marshall Space Flight Center • MSFC, Alabama 35812

February 1995

TABLE OF CONTENTS

	Page
I. INTRODUCTION	1
II. RESIDUAL FLEXIBILITY ANALYTICAL APPROACH	8
III. RESIDUAL FLEXIBILITY MODAL TEST APPROACH.....	11
IV. LEAST-SQUARES CURVE FIT OF RESIDUAL FUNCTION.....	14
V. APPLICATION TO BEAM WITH APPENDAGE	16
VI. APPLICATION TO PALLET SIMULATOR.....	29
VII. CONCLUSION.....	39
REFERENCES.....	40
APPENDIX A – PROGRAM MK_Phi_FRF.m	41
APPENDIX B – PROGRAM rbf.m.....	45
APPENDIX C – PROGRAM res.m.....	49
APPENDIX D – FUNCTION Eign.Sol2.m.....	53

LIST OF ILLUSTRATIONS

Figure	Title	Page
1.	Fixed-base modal test stand	2
2.	SSCMP fixed-base modal test.....	4
3.	Mass additive modal test.....	5
4.	Structures subject to residual modal testing.....	6
5.	Payload installed in the space shuttle.....	7
6.	Test-generated residual function	14
7.	Theoretically generated residual function	15
8.	Beam with trunnion attachment test article.....	18
9.	Free-free modal test of beam	19
10.	Test drive-point FRF for beam.....	21
11.	Synthesized drive-point FRF for beam	22
12.	Overlay of test and synthesized drive-point FRF's for beam	23
13.	Residual function	24
14.	Direct curve fit of residual function	25
15.	Weighting function for beam	26
16.	Weighted curve fit of residual function for beam	27
17.	Theoretically generated residual function from beam model	28
18.	Space shuttle pallet simulator	30
19.	Modal test setup and test equipment	32
20.	Free-free modal test configuration	33
21.	Overlay of test and synthesized drive-point FRF's for pallet simulator	34
22.	Residual function for pallet simulator.....	35
23.	Weighting function for pallet simulator	36
24.	Weighted curve fit of residual function for pallet simulator.....	37

LIST OF TABLES

Table	Title	Page
1.	Correlation of beam model and theoretical solution	17
2.	Comparison of beam model and test data	20
3.	Residual flexibility curve fitting errors for beam.....	29
4.	Correlation results for pallet simulator	38
5.	Curve fitting errors of pallet simulator residual flexibility	38

LIST OF SYMBOLS

<u>Term</u>	<u>Description</u>
A	transformation matrix, real component matrix
a	real part of residual function
B	damping coefficient
b	imaginary part of residual function
Φ	eigenvector
F	force (no subscript external force)
G	MacNeal: deflection influence coefficient matrix, Rubin: flexibility matrix
\bar{G}_{cc}	G with all boundary degrees of freedom restrained
H	inertial coefficient
i	imaginary indicator
M	mass matrix
Q	generalized displacements
U	physical coordinate displacements
X	matrix containing unknown residual mass and flexibility
Y	frequency response function
ω	frequency

Subscript

a	measured (test generated)
c	constrained
cc	free coordinates
ci	at connection point
cs	coupling of free and redundant coordinates

f	flexible body
i	degree of freedom, inertia
N	retained modes
R	rigid body
ss	redundant coordinates
ρ	residual

Superscript

m	modal representation
r	residual
T	transpose
-1	inverse
$(1),(2)$	order
\cdot	first time derivative
$\ddot{}$	second time derivative
$'$	particular or selected

TECHNICAL MEMORANDUM

STATISTICALLY GENERATED WEIGHTED CURVE FIT OF RESIDUAL FUNCTIONS FOR MODAL ANALYSIS OF STRUCTURES

I. INTRODUCTION

In industry, the use of analytical tools to aid in design and analysis of a product is greatly increasing. The type of tools vary depending on the type of analysis and application of the final product. In recent years, the method of finite element analysis (FEA), which is a mathematical representation, has become an industry-wide accepted tool. FEA, which is a reduction of an infinite system to a finite one, is an approximation of the actual system. FEA can be applied to a variety of problems, such as stress analysis, thermal analysis, fluid flow, dynamics, etc.

In the area of dynamics, an FEA can be used to determine the natural frequencies and mode shapes of a structural model. If the frequency of a forcing function is the same as one of the structure's natural frequencies, the dynamic characteristics of the structure can produce increased elastic deformation of the structure's material, causing fatigue, resulting in the destruction of the structure. Since the FEA only approximates the dynamic characteristics of the structure, it is important to eliminate any additional error that may be incorporated into the mathematical model.

Errors arise in two areas: the modeling of the structure (creating the finite element model (FEM)) and fabricating the structure. When creating the FEM, simplifying assumptions lead to errors. In the fabrication of the structure, exact reproduction of the design drawings is impossible. Variations in thicknesses of machined parts and limits on tolerances can change the final characteristics of the structure. The process of eliminating the errors in a mathematical model is known as correlation. Correlation involves modifying the model to match the results obtained from testing the physical structure.

Once a mathematical model has been correlated, it can be used to predict, with increased confidence, the response of the structure under expected loadings. How a structure will behave in its operational environment is of great importance. The structure interacts with the environment at its interface points. In structural dynamics, the interface points are where the object receives its excitation and transmits its vibrational loads back to the environment. The interface points are areas where a high level of confidence in the mathematical model representation is critical.

Dynamically correlating a mathematical model with test results requires a modal test of the physical structure. The type of modal testing performed depends on the structure and the type of interfacing the structure has with its environment. The two most commonly performed modal tests are the free-free and fixed-base tests. For structures with constrained (fixed) interfaces, historically the fixed-base modal test was performed. Fixed-base testing has many drawbacks for large structures such as interface simulation and cost. Extreme difficulties arise when trying to simulate the interfaces between the structure and its environment when only selected degrees of freedom (DOF) are to be constrained. The cost involved in design and construction of a test stand can become prohibitive.

As stated previously, fixed-base tests of large structures are extremely difficult and expensive. As an example, the Boeing Company in Huntsville, AL, designed and built a large test stand to perform modal tests on the space station modules in a fixed-base configuration (fig. 1). Extreme care was taken

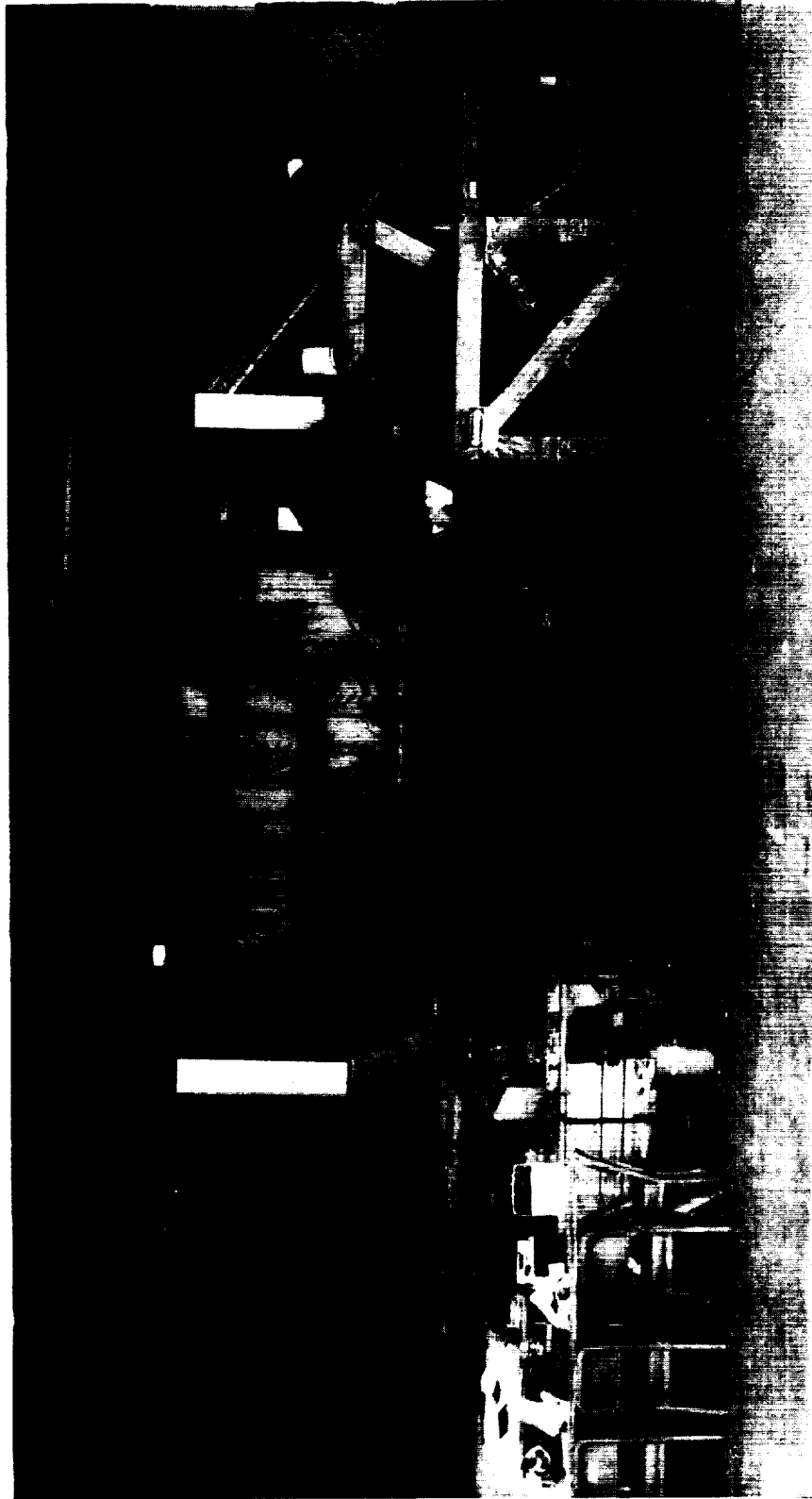


Figure 1. Fixed-base modal test stand.

in the design of the test stand to keep the dynamic characteristics of the stand from corrupting the test data. A fixed-base modal test of the space station common module prototype (SSCMP), built by Boeing for preliminary testing, was conducted in the test stand for test stand checkout (fig. 2). The module has seven DOF where it interfaces with its environment. An elaborate off-loading system, which utilized air bags to lift the trunnions off the lower bearing surface to reduce the contact friction, was used to allow movement in the remaining DOF at the interface points.

The fixed-base modal test of the SSCMP failed. The off-loading system did not free the remaining DOF at the interface locations. Boeing is presently redesigning the areas around the interface points of the test stand. Over a million dollars has already been spent on the test stand and its design. It can easily be seen why an alternative modal testing technique is greatly needed.

Due to simulation problems and economic pressures, alternative modal testing methods are being considered. Mass additive and residual flexibility testing methods are two such methods. The mass additive method involves the attachment of masses to the interface DOF which helps to exercise the interface modes, aiding in constrained modes prediction (fig. 3). References 1, 2, and 3 discuss the implementation of the method along with its advantages and disadvantages.

The residual flexibility modal testing method consists of measuring the free-free natural frequencies and mode shapes along with the interface frequency response functions (FRF's). Analytically, the residual flexibility method has been investigated in detail,⁴⁻⁶ but has not been implemented extensively for model correlation due to difficulties in data acquisition. In recent years, improvement of data acquisition equipment has made possible the implementation of the residual flexibility method.⁷⁻¹¹ The residual flexibility modal testing technique is applicable to a structure with distinct points (DOF) of contact with its environment. Examples are shown in figure 4.

Payloads of the space shuttle are structures that have distinct interface points at its support trunnions and are prime candidates for the residual flexibility modal test method (fig. 5). Since the *Challenger* shuttle incident in 1986, NASA requires that all final loads analysis of the payload be performed with a mathematical model that has been correlated to modal test data. A load analysis consists of coupling the payload's mathematical model to a space shuttle mathematical model, dynamically exciting it analytically, and evaluating the response loads the payload exerts on the shuttle during takeoff, on orbit, and landing configurations. Usually the mode shapes that produce the highest value in a load analysis are the modes that excite the bending of the trunnions and exercise their local stiffness. Johnson Space Center (JSC), which is responsible for the shuttle fleet, requires the mathematical model to be correlated, up to 35 Hz, to a modal test data of a fixed-base configuration. A fixed-base configuration involves rigidly constraining the interface DOF. JSC requires this configuration because the exact interface point characteristics on the shuttle are unknown. These characteristics also change when different payloads are placed in the cargo bay. JSC also chose the fixed-base test since the corresponding modes are required in a loads analysis.

If the payload was tested in a free-free configuration, the bending stiffness of the trunnions would not be measured (trunnion natural frequencies are usually greater than 150 Hz). Measuring the free-free bending stiffness of the trunnions in a free-free modal test and correlating the mathematical model are not sufficient to predict constrained modes.⁷ In addition to measuring the bending stiffness of the trunnions, the residual flexibility modal testing method also measures the contributions of the higher order modes.

The study of the implementation and analysis usability of the residual flexibility modal test technique is being conducted at the NASA/Marshall Space Flight Center (MSFC) in Huntsville, AL.

ORIGINAL PAGE
BLACK AND WHITE PHOTOGRAPH

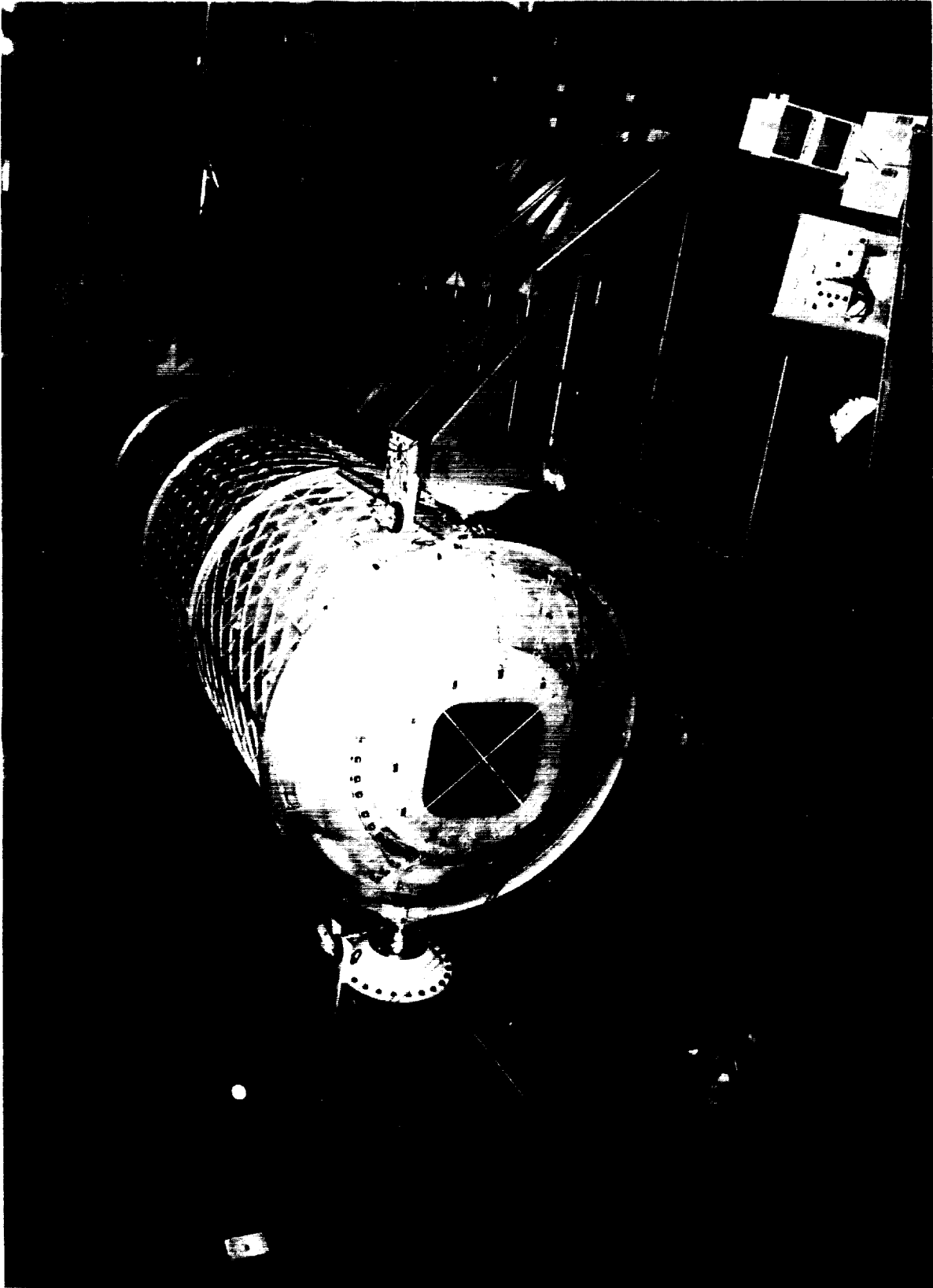


Figure 2. SSCMP fixed-base modal test.

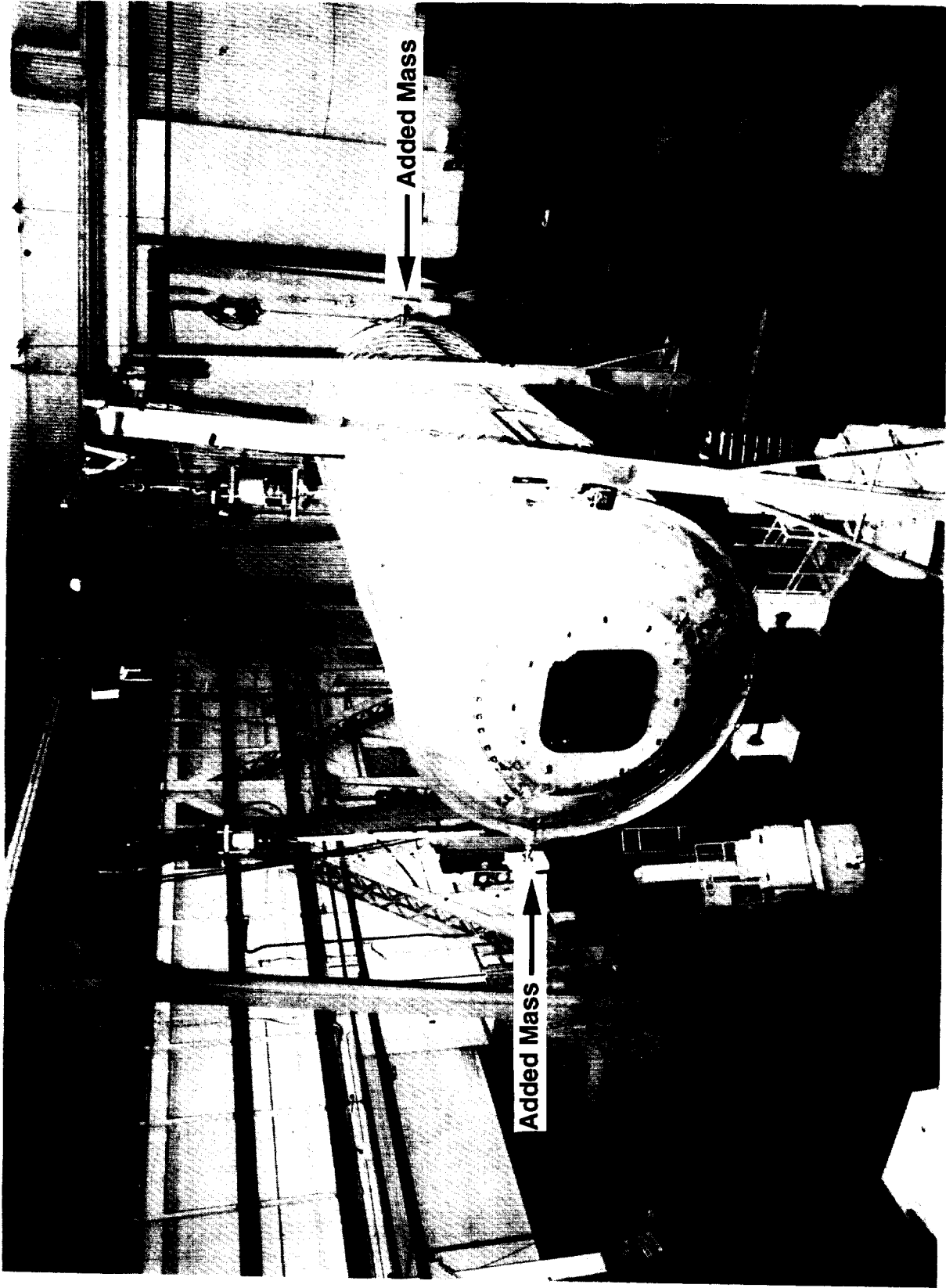


Figure 3. Mass additive modal test.

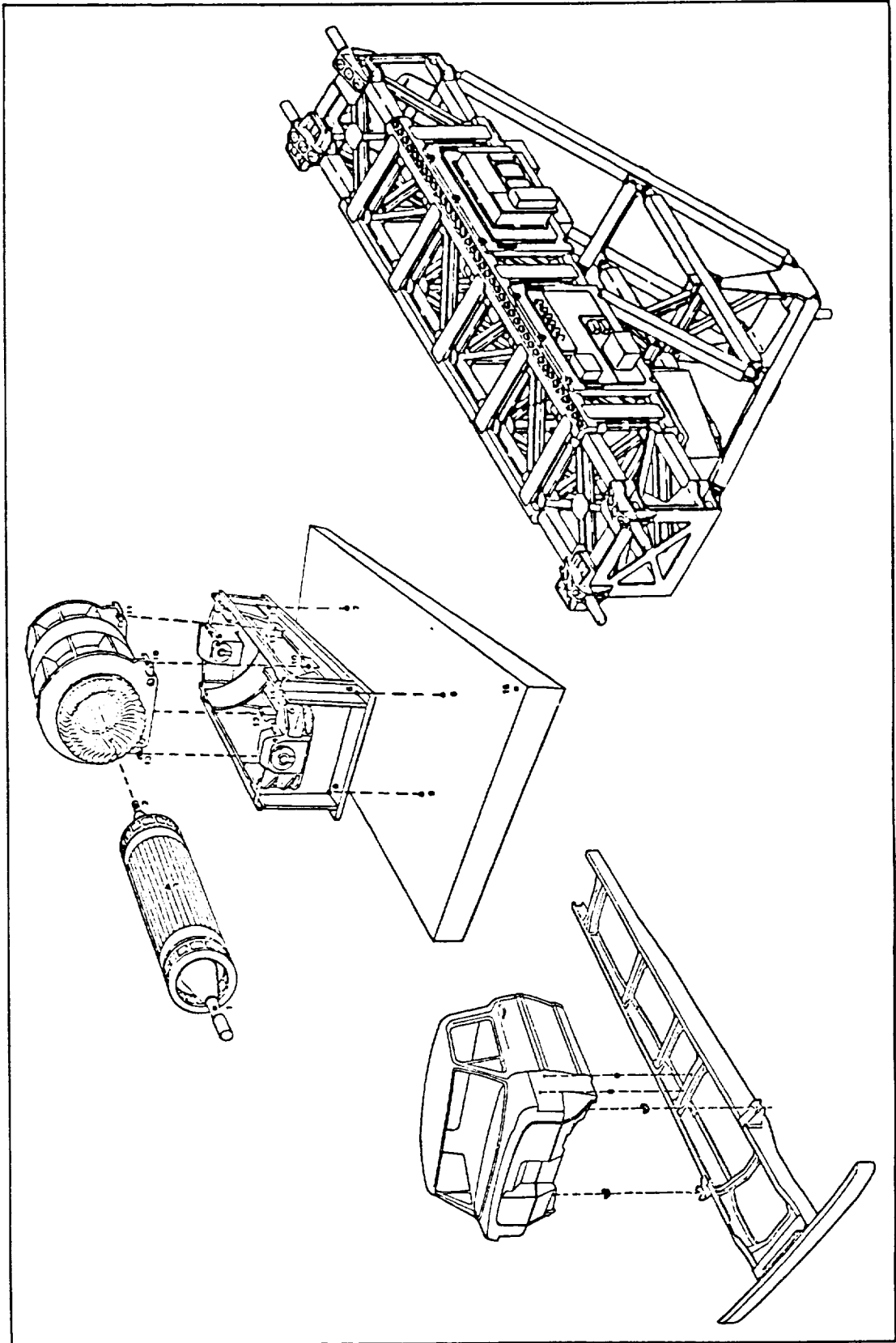


Figure 4. Structures subject to residual modal testing.

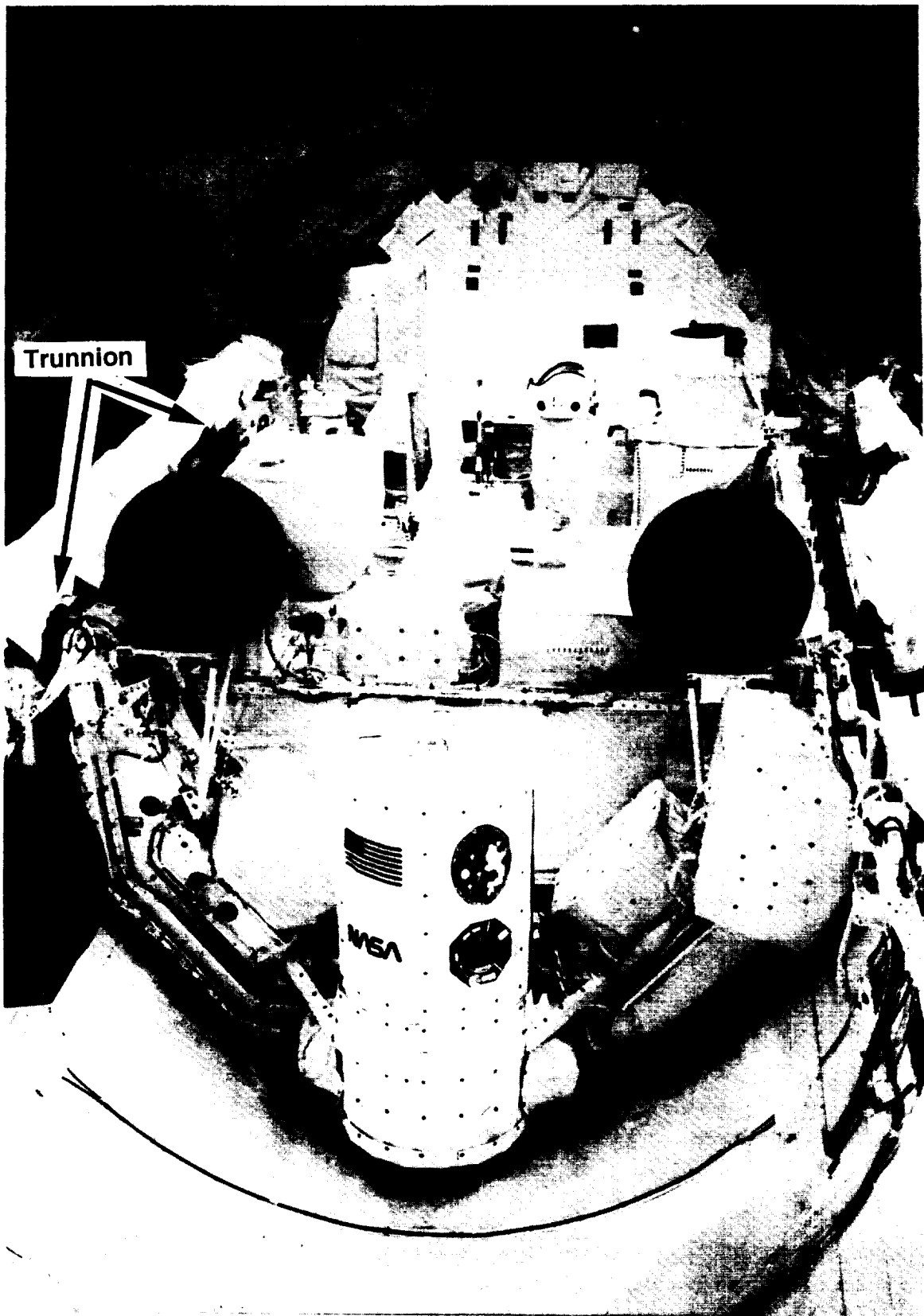


Figure 5. Payload installed in the space shuttle.

A research task entitled “Residual Flexibility In-House Implementation Study” is being conducted by the Dynamics and Loads Branch and the Experimental Dynamics Test Branch at MSFC. During this study, a problem was encountered when trying to extract the residual flexibility from the test data.

This report discusses the development of a statistically generated weighted curve fit for assisting in the analysis of the residual flexibility test data. First, a brief analytical discussion is presented, followed by an explanation of the generation of the residual function from test data, and the implementation of the statistically generated weighted curve fit to extract the residual terms. The residual flexibility method is then applied to a simple beam with a trunnion type interface and a space shuttle pallet simulator. The residual terms are then compared to a mathematical model taken as the exact answer and percentage errors are presented.

II. RESIDUAL FLEXIBILITY ANALYTICAL APPROACH

The residual technique, which was first developed by MacNeal,⁵ incorporates the use of the higher frequency mode effects (residual modes) which are not directly used in the analysis to improve the reduced mathematical model. MacNeal derives statically the deflection influence coefficient matrix, G , associated with the free coordinates, G_{cc} , and the redundant support coordinates, G_{ss} , for the determinate restrained DOF, which is given by

$$G = \begin{bmatrix} G_{cc} & G_{cs} \\ G_{cs}^T & G_{ss} \end{bmatrix}, \quad (1)$$

where G_{cs} is the coupling of the redundant support and free coordinates.

MacNeal further defines the deflection influence coefficient matrix with all boundary DOF restrained as,

$$\bar{G}_{cc} = G_{cc} - G_{cs} G_{ss}^{-1} G_{cs}^T. \quad (2)$$

Next, casting the modal representation in a manner similar to the deflection influence coefficient matrix, equation (1), gives,

$$G_{cc}^m = \Phi_{ci} K_i^{-1} \Phi_{ci}^T, \quad (3)$$

where the Φ_{ci} term contains the eigenvectors at the connection point and K_i is the corresponding stiffness matrix. Subtracting equation (3) from equation (2) produces the residual flexibility matrix,

$$G_{cc}^r = \bar{G}_{cc} - G_{cc}^m. \quad (4)$$

This approach is difficult to implement the way it was derived. MacNeal only makes use of the residual stiffness and neglects the mass and damping terms.

Rubin⁴ starts with the same statics approximation as MacNeal, but formulates the residual flexibility in a different way. The statics approximation for a discrete system is written as,

$$U_f^{(1)} = GF \quad , \quad (5)$$

where $U_f^{(1)}$ is the displacement matrix of the flexible body, F is the external force vector, and G is the flexibility matrix of the free body.

The flexibility matrix is defined as the inverse of the stiffness matrix, $G = K^{-1}$. For the unconstrained case, the stiffness matrix is singular and G cannot be computed directly. For the constrained case, G_c can be calculated from K_c (constrained stiffness), $G_c = K_c^{-1}$. G and G_c differ by the rigid-body inertia forces of the system. When the system is unconstrained, the system has elastic and rigid-body movement. The rigid-body movement of the system has inertia forces associated with its mass. When the system is constrained, the elastic motion of the system is present but the rigid-body movement is missing. A way to incorporate the free-body inertia into G_c is needed to produce an equivalent unrestrained flexibility matrix. Rubin writes the displacement of the physical coordinates due to generalized rigid-body displacements as,

$$U_R = \Phi_R Q_R \quad , \quad (6)$$

with the differential equation relating the generalized rigid-body displacements to the external forces being,

$$M_R \ddot{Q}_R = \Phi_R^T F \quad , \quad (7)$$

where $M_R = \Phi_R^T M \Phi_R$ is the rigid-body generalized mass, and M is the physical mass matrix. The sum of the external forces, F , and the inertia forces, F_i , can be expressed as,

$$F + F_i = F - M \ddot{U}_R = AF \quad , \quad (8)$$

where

$$A = I - M \Phi_R M_R^{-1} \Phi_R^T \quad .$$

The constrained equation for the first-order statics approximation for a discrete system, where G_c is the constrained-body flexibility matrix, is stated as,

$$U_c^{(1)} = G_c (F + F_i) = G_c AF \quad . \quad (9)$$

Rubin further explains that this is an unusual statics problem where the flexibility matrix G_c is singular and, in general, nonsymmetric.

By adding certain generalized rigid-body displacements, Q_R' , to the constrained deflection given in equation (9), the first-order flexible-body displacements can be written as,

$$U_f^{(1)} = U_c^{(1)} + \Phi_R Q_R' \quad . \quad (10)$$

Defining the $U_R^{(1)}$ in a way that it is orthogonal to the rigid-body modes (i.e., removing any rigid-body contributions) gives,

$$\Phi_R^T M [U_c^{(1)} + \Phi_R Q_R'] = 0 \quad . \quad (11)$$

Solving for Q_R' , substituting into equation (10), and using the relationship $M_R = \Phi_R^T M \Phi_R$, the free-body symmetric flexibility matrix, G , for the first-order approximation is,

$$U_f^{(1)} = GF \quad , \quad (12)$$

where

$$G = A^T G_c A \quad ,$$

and A is given in equation (8). Note that G is singular since G_c is singular.

The second-order statics approximation is obtained by including the inertial and damping forces of the first-order deflections in equation (9),

$$U_f^{(2)} = G_c A \left[F - M \ddot{U}_f^{(1)} - C \dot{U}_f^{(1)} \right] \quad , \quad (13)$$

and in a similar way removing the rigid-body contributions,

$$U_f^{(2)} = GF - H \ddot{F} - B \dot{F} \quad , \quad (14)$$

where

$$H = GMG \quad ,$$

$$B = GCG \quad ,$$

where H and B are the inertial and damping coefficient matrices, respectively. Note that the inertial and damping coefficients are calculated from pre- and postmultiplication of G found from the first-order approximation. In addition, H and B are symmetric since G , M , and C are symmetric.

At this point, the approximate deflection for the entire flexible body for first and second orders are given by equations (12) and (14), respectively. By removing the retained modes (measured modes) in the above equations, the residuals are obtained.

The residuals for the first-order static equation are,

$$U_{f\rho}^{(1)} = G_\rho F \quad , \quad (15)$$

where

$$G_\rho = G - G_N, \quad G_N = \Phi_N K_N^{-1} \Phi_N^T,$$

and the mode shape and generalized stiffness matrices of the retained modes are Φ_N and K_N , respectively. Similarly, the second-order formulation is expanded from the first-order statics equation by including correction terms,

$$U_{f\rho}^{(2)} = G_\rho F - H_\rho \ddot{F} - B_\rho \dot{F}, \quad (16)$$

where

$$H_\rho = H - H_N, \quad H_N = G_N M G_N,$$

$$B_\rho = B - B_N, \quad B_N = G_N C G_N.$$

G_ρ is given in equation (15), H and B are given in equation (14). In addition, by making use of modal orthogonality, the residual mass and damping can be computed by pre- and postmultiplying the full mass and damping matrices, respectively,

$$H_\rho = G_\rho M G_\rho, \quad (17)$$

$$B_\rho = G_\rho C G_\rho. \quad (18)$$

One now has the equations to compute the residual flexibility (stiffness), residual mass, and residual damping terms for a mathematical model of a structure. Note: Martinez⁶ restated the equations to determine the residual terms in a form which is similar to the Craig-Bampton formulation.¹² The Craig-Bampton formulation is used widely in loads analysis.

III. RESIDUAL FLEXIBILITY MODAL TEST APPROACH

Modal testing of a structure is required for correlation of a mathematical model of the structure. A mathematical model correlated to a free-free modal test is not accurate enough to predict the constrained mode shapes, as discussed in reference 7. The model must also be correlated to at least the residual flexibility terms, which in this study represents the flexibility around the interface points. In this procedure, the determinations of the test-generated $H_{\rho a}$, $B_{\rho a}$, and $G_{\rho a}$, the residual mass, damping, and flexibility, respectively, are used for comparison to the mathematical model's residual terms found in equations (15) and (16).

The residual flexibility modal test consists of first measuring the free-free modes in the frequency range of interest. This includes the rigid-body modes (in the analysis, the mathematical model's rigid-body modes can be used if the total mass and its distribution in the model are relatively accurate). The measured free-free modes are used to correlate the global modes of the mathematical model which can be performed at a later time. The structure is then excited at the points where it interfaces with its environment (boundary or interface DOF).

Exciting each interface point individually, the response due to the excitation is measured at the same location and in the same direction as the excitation, producing a drive point FRF. Modal parameters (mode shapes and natural frequencies) are then extracted from the FPF obtained from the free-free modal test. From the modal parameters, synthesized FRF's are generated and then subtracted from the corresponding drive point test FRF's. The remaining functions are called the residual functions. The residual flexibility term is defined as the value of the residual function evaluated at zero frequency (constant term in the curve fit equation which will be discussed in detail later). The residual mass is the curvature of the residual function (second-order term in the curve fit equation) in the displacement/force domain. Finally, the residual damping (first-order term in the curve fit equation) is equated to the damping obtained from the modal test. The residual terms are then compared to the corresponding theoretical residual terms. The mathematical model is modified to match the test results. Once the mathematical model is correlated to the free-free mode shapes and the residual terms, it can be used to predict the constrained mode shapes.⁷

In this derivation, the residual terms will be extracted from the FRF in the displacement/force domain instead of the usual acceleration/force domain. Using the displacement/force domain allows easier recognition of the characteristics of the residual function and the residual flexibility term.

Y_a , the FRF matrix is represented in the form,

$$U_a(\omega) = Y_a(\omega)F_a(\omega) \quad . \quad (19)$$

The elements of the main diagonal of $Y_a(\omega)$ are the drive point FRF's at each interface point and direction. One column of $Y_a(\omega)$ is the result of exciting one interface point and measuring the response at that point and all the other interface points and directions. $Y_a(\omega)$ can be thought of as a three-dimensional matrix with two dimensions of the matrix defining the location and direction of a particular FRF. The third dimension along the ω axis represents the actual values of the FRF's. The FRF's are only measured in the frequency range of interest. The unmeasured range will produce the residual function.

The technique for obtaining the response functions is left up to the test engineer. Care must be taken to accurately measure the first antiresonance of the response function. An accurate determination of the first antiresonance is the governing factor in determining the residual flexibility term. The first antiresonance is the lowest in frequency distinguishable characteristic of the FRF and, since the residual flexibility term is evaluated at zero frequency of the residual function, any shift in the first antiresonance significantly affects the residual flexibility term.

The modal parameters are extracted from the FRF's producing retained natural frequencies and mode shapes. These natural frequencies and mode shapes together with the rigid-body modes are subtracted from the corresponding FRF to produce the residual function coefficients, $Y_{\rho a}(\omega)$,

$$Y_{\rho a}(\omega) = Y_a(\omega) - \Phi_{Ra} Y_R \Phi_{Ra}^T - \Phi_{Na} Y_N \Phi_{Na}^T \quad , \quad (20)$$

where Φ_{Ra} and Φ_{Na} are the rigid-body and retained free-free modes, respectively, and,

$$Y_R = -\frac{1}{\omega^2} M_R^{-1} \quad ,$$

$$Y_N = \Lambda_N^{-1} M_N^{-1} ,$$

$$\Lambda_N = -\omega^2 + i2\zeta_n \omega \omega_n + \omega_n^2 .$$

Y_R and Y_N are the modal dynamic flexibility matrices for classically damped modes. The rigid-body mass and retained elastic-body modal mass, M_R and M_N , respectively, are identity matrices if the modes are initially normalized to modal mass.

Once the residual function is determined, the residual terms (flexibility, mass, and damping) are extracted. A second-order form, similar to equation (16), is used to estimate the residual function,

$$Y_{\rho a}(\omega) = \omega^2 H_{\rho a} - i\omega B_{\rho a} + G_{\rho a} . \quad (21)$$

As can be seen, the residual function $Y_{\rho a}(\omega)$ is a complex number, and the real and imaginary components can be separated. $Y_{\rho a}(\omega)$ is in the form,

$$Y_{\rho a}(\omega) = a + bi , \quad (22)$$

where

$$a = \text{Real}(Y_{\rho a}(\omega)) , \quad b = \text{Imag}(Y_{\rho a}(\omega)) .$$

Equating equations (21) and (22) gives,

$$a + bi = (\omega^2 H_{\rho a} + G_{\rho a}) - i\omega B_{\rho a} . \quad (23)$$

Equating the imaginary components, the residual damping term is found to be,

$$B_{\rho a} = -\frac{b}{\omega} . \quad (24)$$

The residual mass and flexibility are determined by equating the real components,

$$a = G_{\rho a} + \omega^2 H_{\rho a} . \quad (25)$$

Rewriting equation (25) in matrix form gives,

$$a = AX , \quad (26)$$

where

$$A = \begin{bmatrix} 1 & \omega_1^2 \\ 1 & \omega_2^2 \\ \vdots & \vdots \\ 1 & \omega_N^2 \end{bmatrix} , \quad X = \begin{bmatrix} G_{\rho a} \\ H_{\rho a} \end{bmatrix} ,$$

and N is the total number of data points. Solving for X gives,

$$X = A^{-1}a , \quad (27)$$

the residual flexibility and the residual mass. Since A is not square, other solution methods must be implemented, such as the pseudoinverse to determine the unknowns, $G_{\rho a}$ and $H_{\rho a}$. These values are compared to the residual terms calculated from the mathematical model for correlation purposes.

IV. LEAST-SQUARES CURVE FIT OF RESIDUAL FUNCTION

The determination of the residual terms (residual mass and flexibility) from the residual function requires a second-order polynomial curve fit of equation (25). The imaginary term has previously been determined, equation (24), and is not included in the curve fit. If the subtraction of the synthesized FRF from the test (measured) FRF was clean (i.e., no ragged data regions), a direct curve fit could be accomplished for equation (27). But due to the errors in the synthesized FRF, the resulting residual function has regions of ragged data (fig. 6). The errors in the synthesized FRF are attributed to the limitation in the evaluation of the modal parameters from the test FRF's.

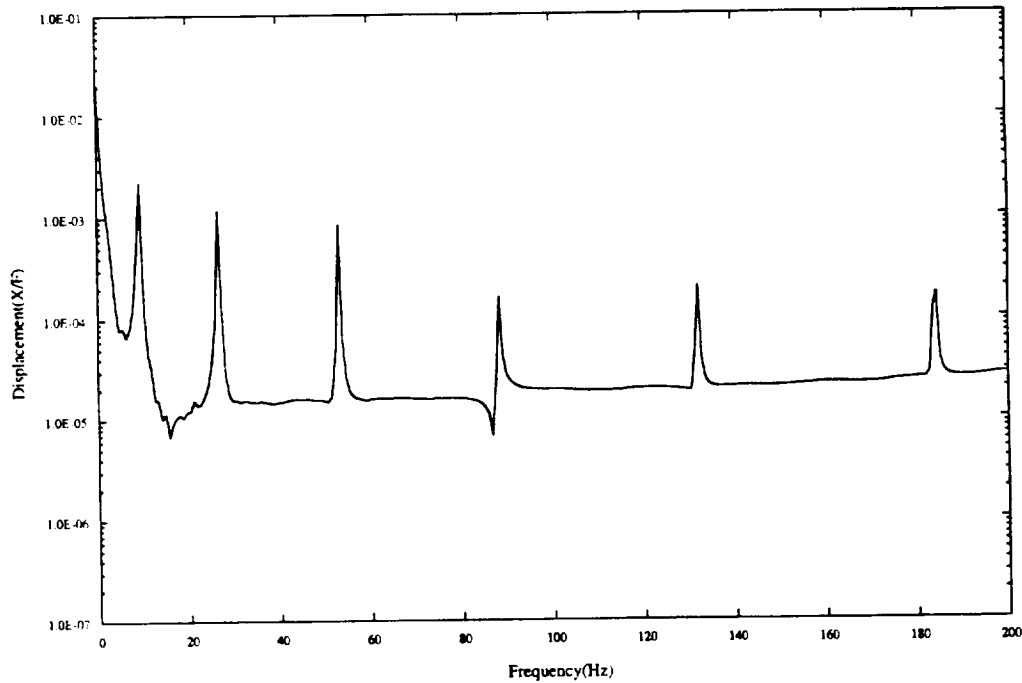


Figure 6. Test-generated residual function.

A theoretical residual function in the displacement/force domain (fig. 7) has the characteristics of a relatively flat line in the lower frequencies and a slight upward curvature in the higher frequency range. These are the characteristics of a second-order equation with only the constant and second power terms (equation (25)). Using these characteristics, a weighted curve fit of the residual function could be used to eliminate the ragged data. A method of determining the weighting function for the curve fit that eliminates any guess work from the analyst is required.

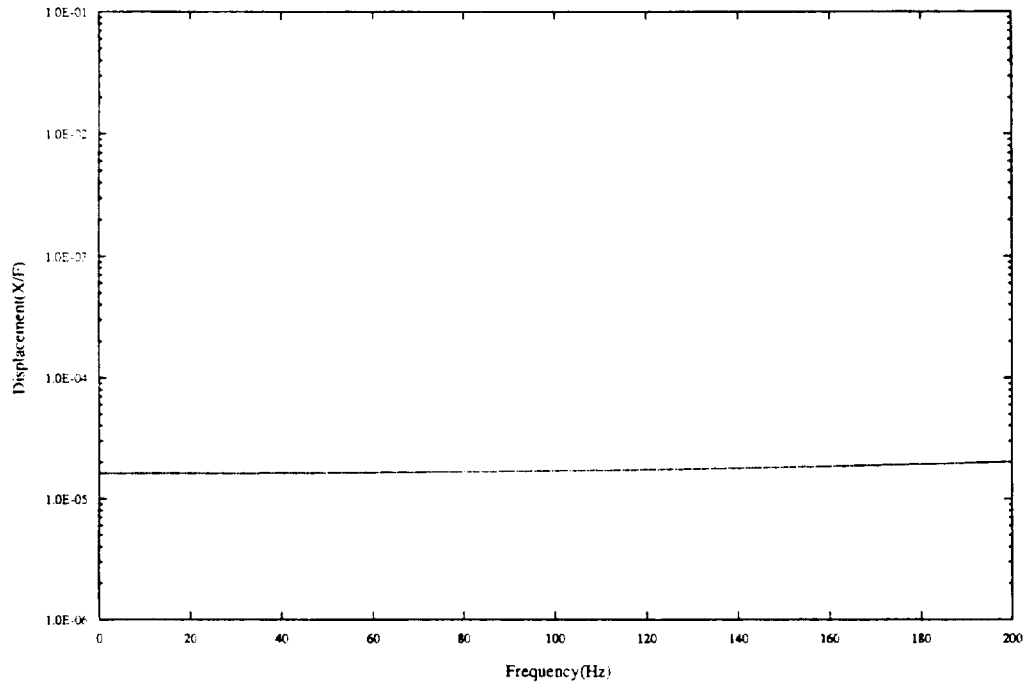


Figure 7. Theoretically generated residual function.

As stated previously, the residual function is relatively flat at the lower frequencies, i.e., the difference (variance) between adjacent data points is small. In the regions of ragged data, the variance between adjacent data is large. When the variance is large between data points, its influence on the curve fit should be minimized. In addition, the data point pairs with small variance should have their influence increased. Since a large variance requires small influence and small variance requires large influence, the inverse of the variance is used to eliminate the regions of ragged data. By taking the inverse of the variance of adjacent data points, a weighting function W , is generated,

$$W(j) = \frac{1}{s^2(j)} = \frac{n-1}{j + \text{int}\left(\frac{n-1}{2}\right) \sum_{i=j-\text{int}\left(\frac{n}{2}\right)}^{j+\text{int}\left(\frac{n-1}{2}\right)} (x_i - \bar{x})^2} \quad (28)$$

where

$$j = \text{int}\left(\frac{n+2}{2}\right), \text{int}\left(\frac{n+2}{2}\right) + 1, \dots, N - \text{int}\left(\frac{n-1}{2}\right),$$

and $s^2(j)$ is the variance,¹³ N is the total number of data points, n is the number of adjacent data points for which the variance is calculated, \bar{x} is the mean of the n adjacent data points for each j , and $\text{int}(\#)$ is the integer part of $\#$ (i.e., $\text{int}(1.5) = 1$).

Forming W into a square matrix is accomplished by setting the main diagonal equal to the weighting function and all other terms equal to zero. The square matrix W must be $N \times N$ in size. When calculating the weighting function, the first and last few data points, depending on the value of n chosen,

will not have a weighting value assigned. Forcing a value of zero at these points will make W be $N \times N$. This can be justified due to the fact that at the extreme limits, data acquisition equipment is not as accurate as in the middle range of the equipment, and the test generated residual function is not as accurate there either. Eliminating these points will have little influence on the curve fit. This is demonstrated in the study on the beam in the following sections with exaggerated data point elimination. In addition, only the weighting values of about two or four data points will be set equal to zero compared to about 250 total data points.

Premultiplying both sides of equation (26) by the weighting function matrix gives,

$$Wa = WAX \quad (29)$$

Multiplying both sides by A^T and solving for X yields,

$$X = (A^TWA)^{-1}A^TWa \quad (30)$$

Since A^TWA is a square matrix, the inverse can be computed directly. In this form, there is no need to normalize the weighting function. The residual terms (residual mass and flexibility), which are contained in X , can be used to correlate the mathematical model.

V. APPLICATION TO BEAM WITH APPENDAGE

One of the simplest structures to model is a straight beam. A theoretical solution for the natural frequencies and mode shapes of an unrestrained (free-free) uniform beam is available.¹⁴ The natural frequencies are given by,

$$f_i = \frac{\lambda_i^2}{2\pi L^2} \left(\frac{EI}{m} \right)^{\frac{1}{2}} ; \quad i = 1, 2, 3, \dots \quad (31)$$

where

$$\lambda_{1,2,3,4,5} = 4.73004074, 7.85320462, 10.9956078, 14.1371655, 17.2787597 \quad ,$$

$$\lambda_i = (2i+1) \frac{\pi}{2} ; \quad i \geq 6 \quad ,$$

and the mode shapes are given by,

$$y_i \left(\frac{x}{L} \right) = \cosh \frac{\lambda_i x}{L} + \cos \frac{\lambda_i x}{L} - \sigma_i \left(\sinh \frac{\lambda_i x}{L} + \sin \frac{\lambda_i x}{L} \right) \quad , \quad (32)$$

where

$$\sigma_{1,2,3,4,5} = 0.982502215, 1.000777312, 0.999966450, 1.000001450, 0.999999937 \quad ,$$

$$\sigma_i = 1.0 ; \quad i \geq 6 \quad .$$

With the “exact” answer available, the mathematical model’s elastic modes can be correlated. Once the model is correlated, the model is said to be exact. Table 1 shows the frequency difference less than one-half percent and modal assurance criteria (MAC) values of 1.00. The MAC is an averaged value for the comparison of the mode shapes in the range from zero to one. A value of one indicates a high degree of similarity between mode shapes.

Table 1. Correlation of beam model and theoretical solution.

Mode Number	Test Frequency (Hz)	Model Frequency (Hz)	Difference (Hz)	Difference (Percent)	MAC
1	9.9764	9.9740	0.024	0.02	1.00
2	27.4715	27.493	-0.0215	0.07	1.00
3	53.8007	53.899	-0.0983	0.18	1.00
4	88.8484	89.097	-0.2486	0.27	1.00
5	132.6023	133.096	-0.4937	0.37	1.00
6	185.0520	185.895	-0.8448	0.45	1.00

The correlated model can be used as a baseline for methodology, program development, and test method evaluation.

For this study, the beam structure was modified by attaching a trunnion simulator to one end (fig. 8). The trunnion simulator was a brass rod with two aluminum plates attached on both ends. The plates were used to connect the brass rod to the beam and to attach the testing instruments. The trunnion simulator gives the beam a distinct stiffness change from the free-free beam. The mass of the trunnion simulator is small relative to the mass of the beam and does not affect correlation to the solution of the theoretical uniform free-free beam.

The free-free modal test hardware setup consists of a Hewlett Packard 3562 for data acquisition. The accelerometer utilized during the model test was a PCB Piezotronics 303A accelerometer. The system was excited with an impact hammer utilizing a PCB Piezotronics 208A03 load cell. Once the measurements were acquired, they were ported to a Hewlett Packard 9000/750 workstation running Leuven Measurement Systems (LMS) MODAL™ package for modal parameter estimation. For ease of testing, the accelerometer was fixed at the interface point and the excitation hammer was moved.

Initially, the beam was tested in a free-free configuration (fig. 9), and the elastic modes were compared to the mathematical model. Table 2 shows the percentage difference between natural frequencies and the MAC values. The measurements and the modal parameter estimation (natural frequencies and mode shapes) of the free-free modal test are verified by the results in table 2.

By exciting the test structure at the point where it interfaces with its environment (the end of the brass rod) and measuring the response at the same location, a drive point FRF in the displacement domain was obtained (fig. 10). The modal parameters were computed for the first six natural frequencies, and a synthesized response function was generated (fig. 11). The first six natural frequencies in the maximum frequency range of 0 to 200 Hz were chosen arbitrarily.

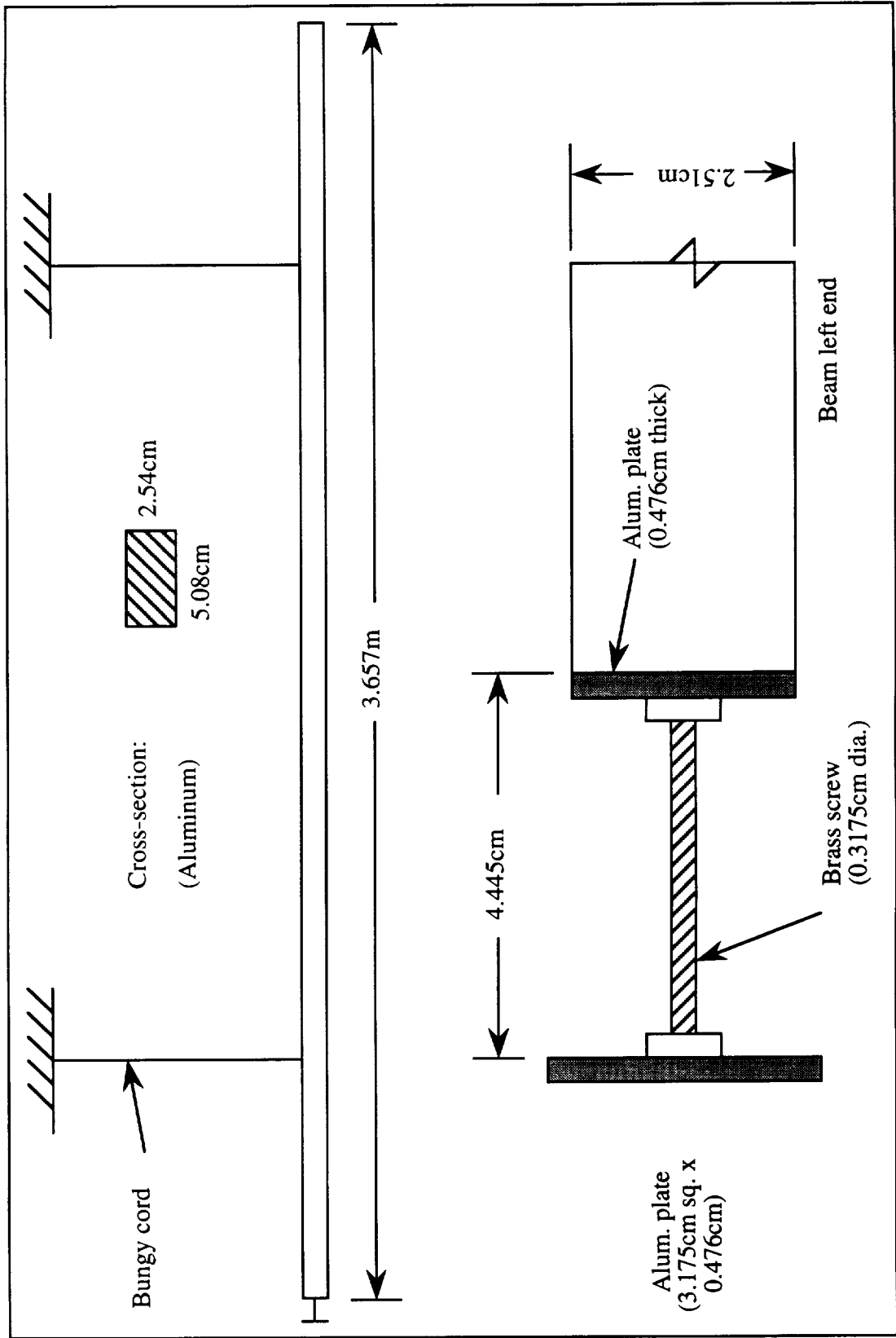


Figure 8. Beam with trunnion attachment test article.

ORIGINAL PAGE
BLACK AND WHITE PHOTOGRAPH

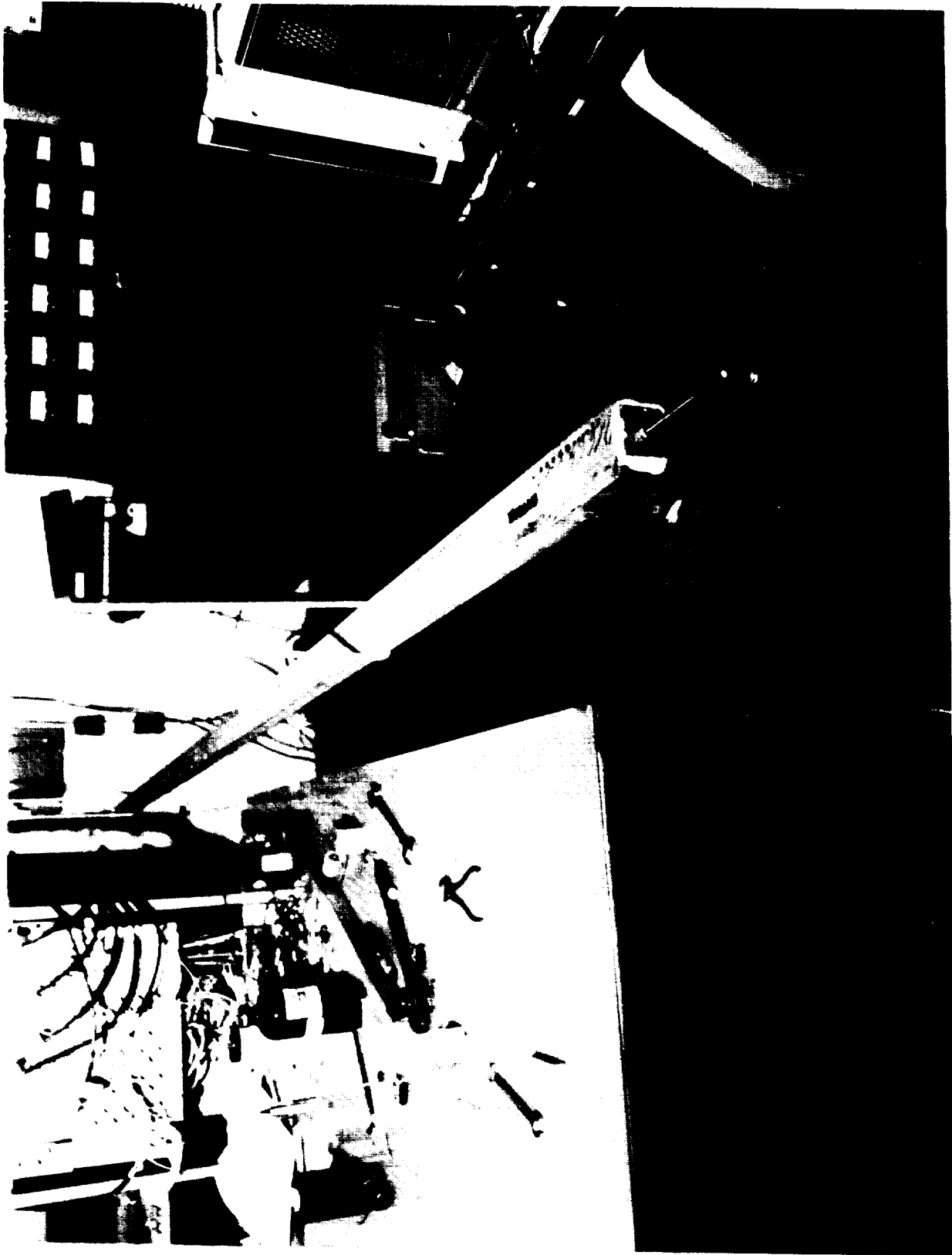


Figure 9. Free-free modal test of beam.

Table 2. Comparison of beam model and test data.

Mode Number	Test Frequency (Hz)	Model Frequency (Hz)	Difference (Hz)	Difference (Percent)	MAC
1	9.9888	9.9764	0.0124	0.12	1.00
2	27.4918	27.4715	0.0203	0.07	1.00
3	53.8265	53.8007	0.0258	0.04	1.00
4	88.9338	88.8484	0.0854	0.09	1.00
5	132.5651	132.6023	-0.0372	0.02	1.00
6	184.7864	185.0520	-0.2656	0.14	1.00

For visual comparison, the drive point and synthesized FRF's have been plotted together in figure 12. The frequency range has been extended to show the relationship between the measured frequencies and the first bending frequency of the trunnion, which occurs at 289 Hz. In an actual test, everything above the cutoff frequency would be unmeasured. The unmeasured region of the FRF is responsible for the residual curve. The subtraction of the test and synthesized response functions producing the residual function can be seen in figure 13. The characteristics of the theoretical residual function are apparent, but with regions of ragged data produced by modal parameter estimations.

A direct curve fit of the residual function was made (fig. 14). The curve fit did not converge on the underlying second-order characteristic curve. Figure 14 was plotted with a linear vertical axis since the value of the curve becomes negative around 150 Hz and the characteristics of the second-order fit can be seen. The ragged data are orders of magnitude higher than the underlying second-order characteristic curve, which throws off the curve fit. By stepping through the data points, a weighting value (inverse of variance) with respect to the neighboring data points can be calculated (equation (28)). The neighboring data points were initially examined in sets of three. It can be seen in figure 15, which contains the weighting and residual functions, that the weighting function has low values where the residual function has regions of ragged data. Another curve fit was performed using the statistically generated weighting function (equation (30)) with highly accurate results (fig. 16).

The exact answers were obtained by equation (16). The same values can be obtained by following the test procedure in generating the residual function. The drive-point FRF is generated by using the elastic modes of the model. Figure 17 shows the residual function generated from the mathematical model. The residual values of $1.6045e-5$ for flexibility and $5.7540e-12$ for mass were compared to the exact answer (mathematical model) and found to have 0.81- and 18.44-percent error, respectively. It has been determined from the research task being performed by MSFC/NASA that the residual mass and damping terms can be neglected in the correlation of the mathematical model, which is used to predict constrained natural frequencies and mode shapes. However, the residual mass term is important in the curve fitting process due to the curvature of the residual function. To verify the process, additional weighting functions and curve fits were performed by varying parameters. The number of adjacent data points was changed to two and four along with the range of the data points for which the weighting functions were computed and applied (table 3).

By varying the upper and lower frequency ranges, an evaluation of the effects of excluding data points in the curve fit process is examined. The changes in the percent error of the frequency range

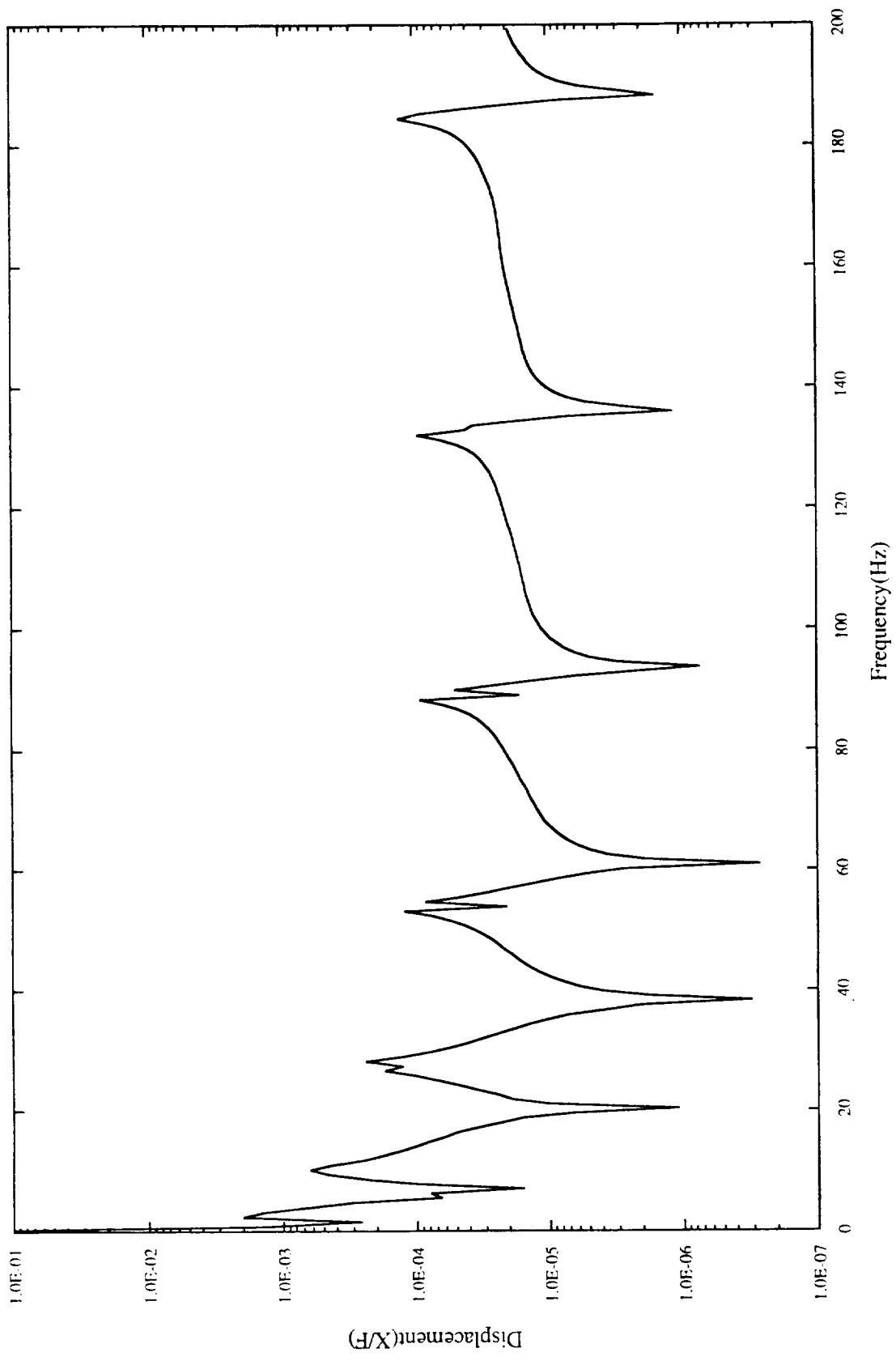


Figure 10. Test drive-point FRF for beam.

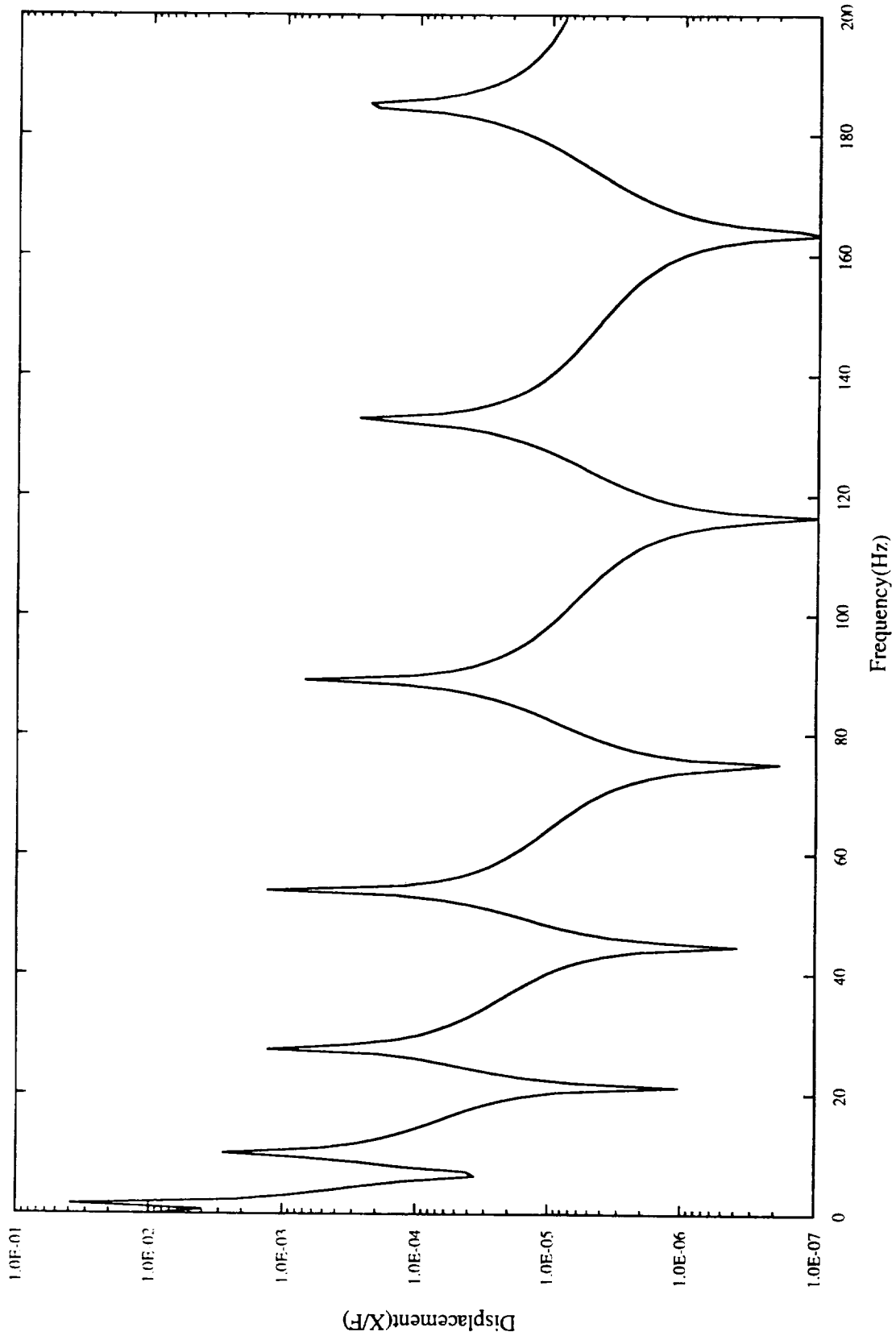


Figure 11. Synthesized drive-point FRF for beam.

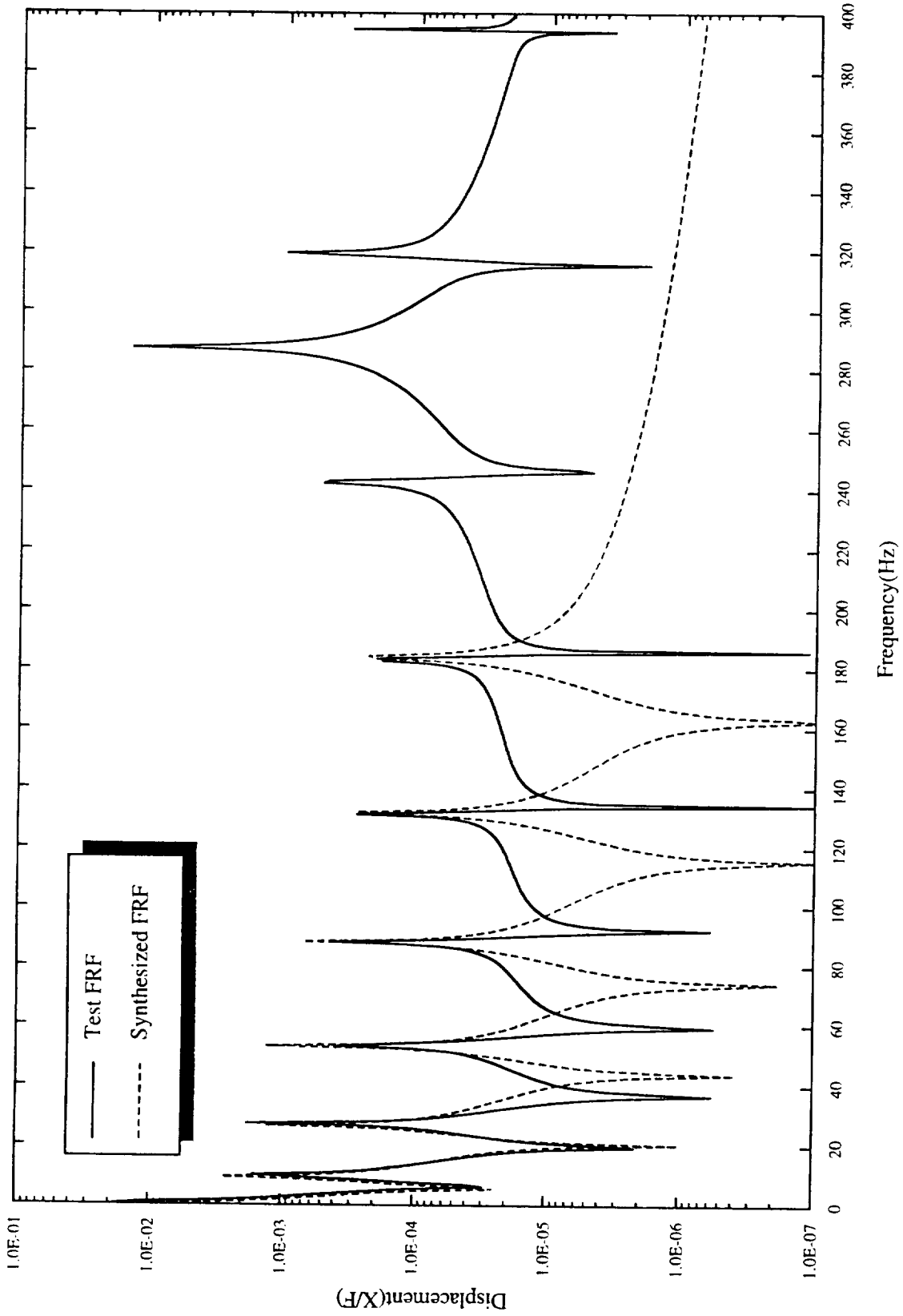


Figure 12. Overlay of test and synthesized drive-point FRF's for beam.

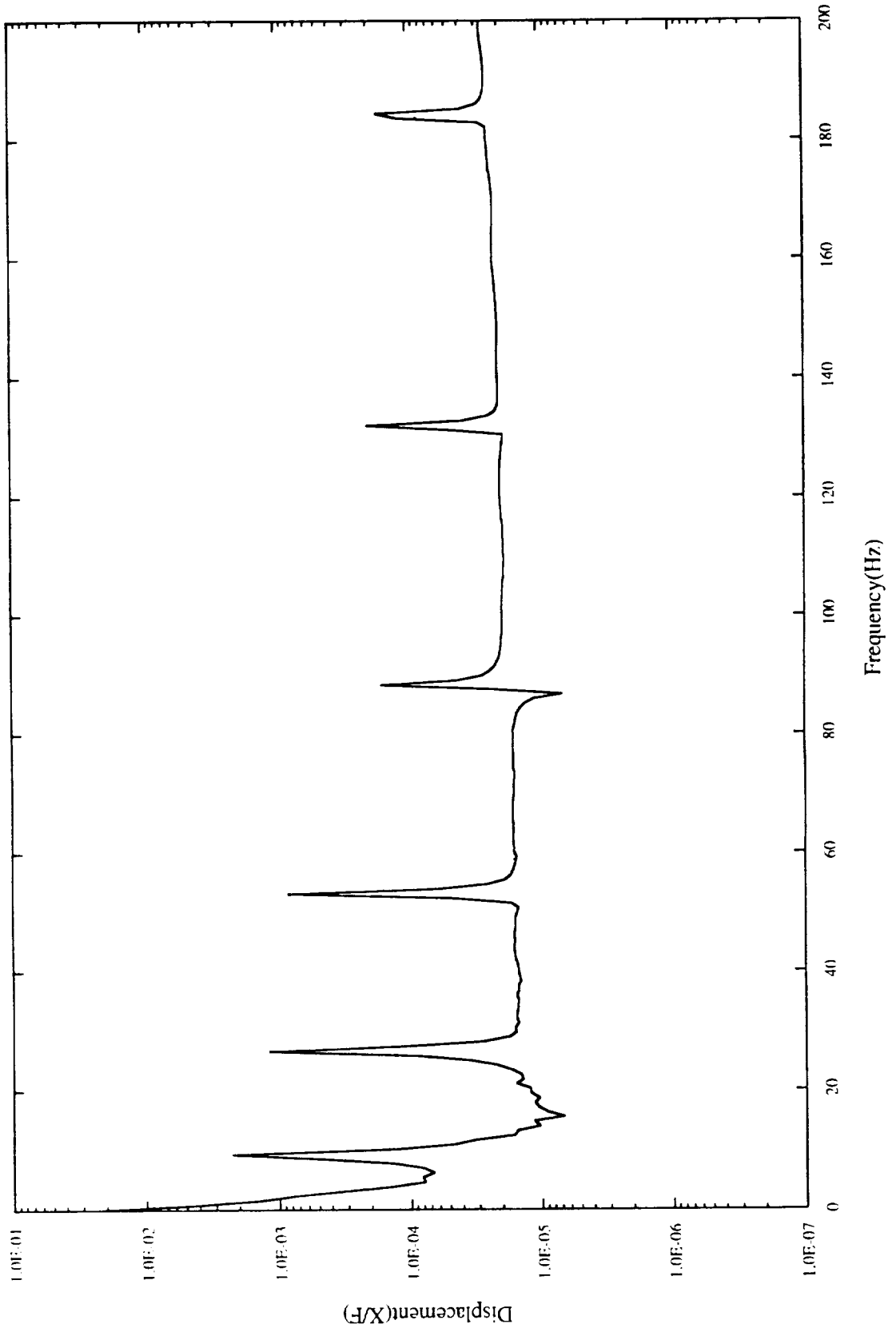


Figure 13. Residual function.

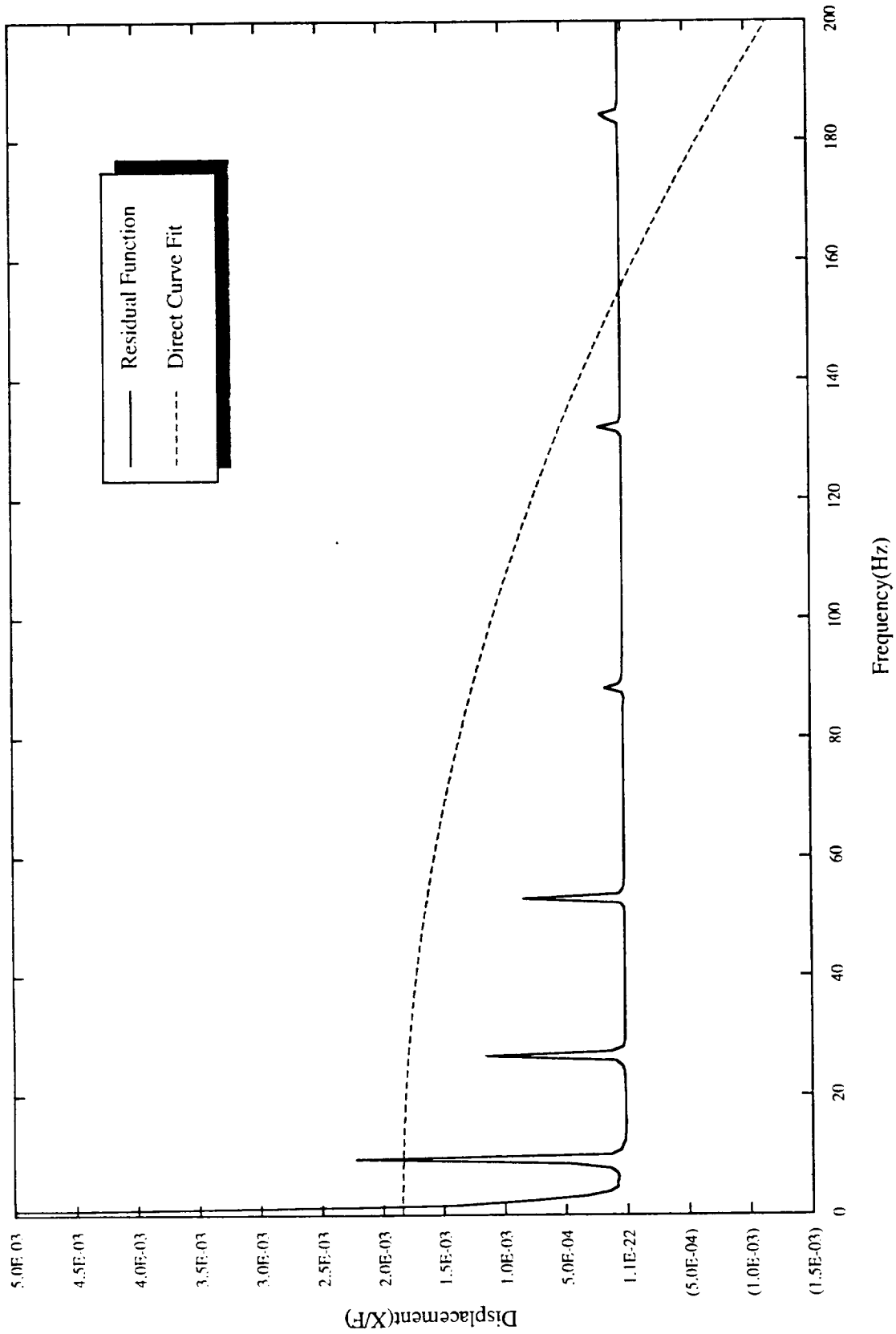


Figure 14. Direct curve fit of residual function.

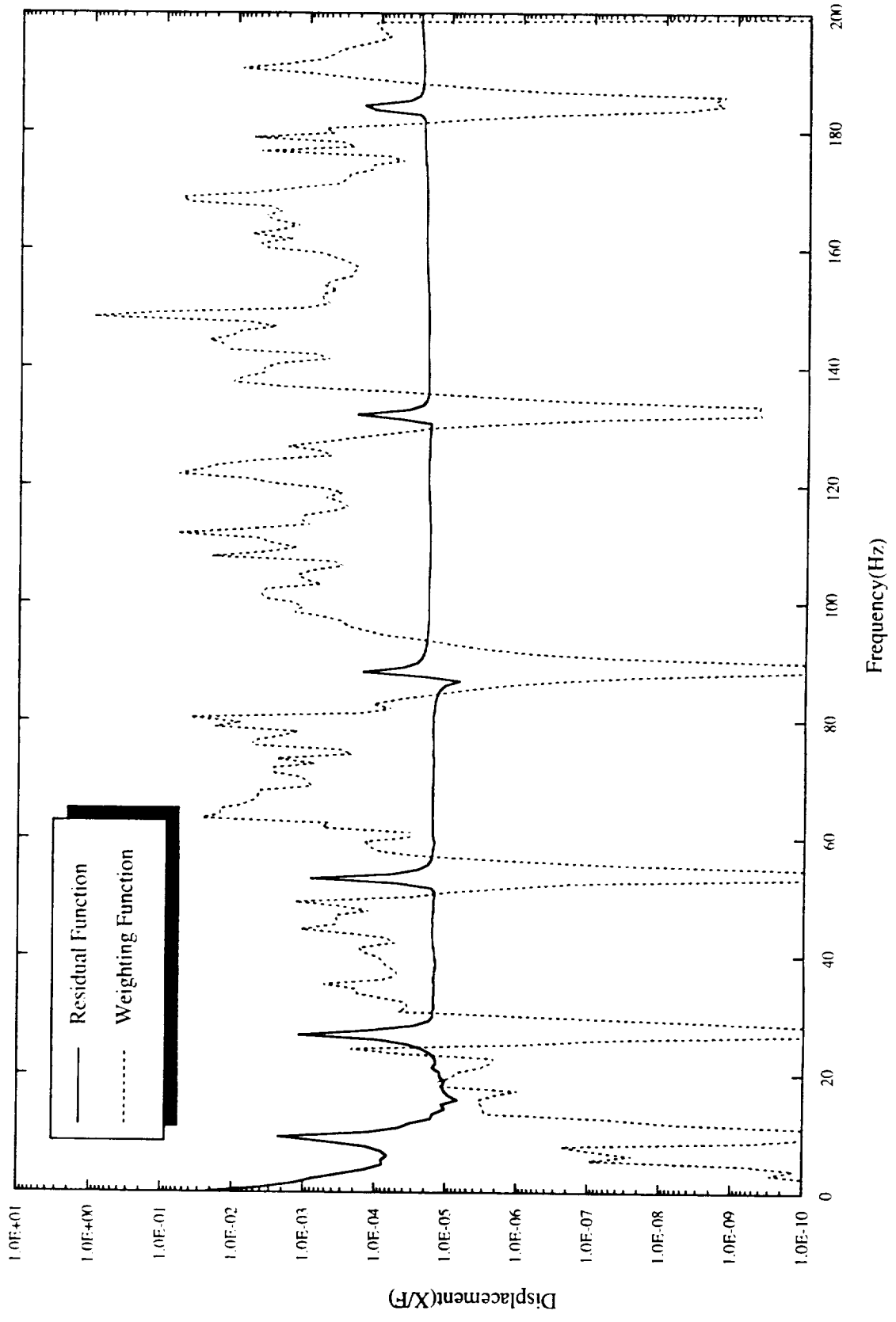


Figure 15. Weighting function for beam.

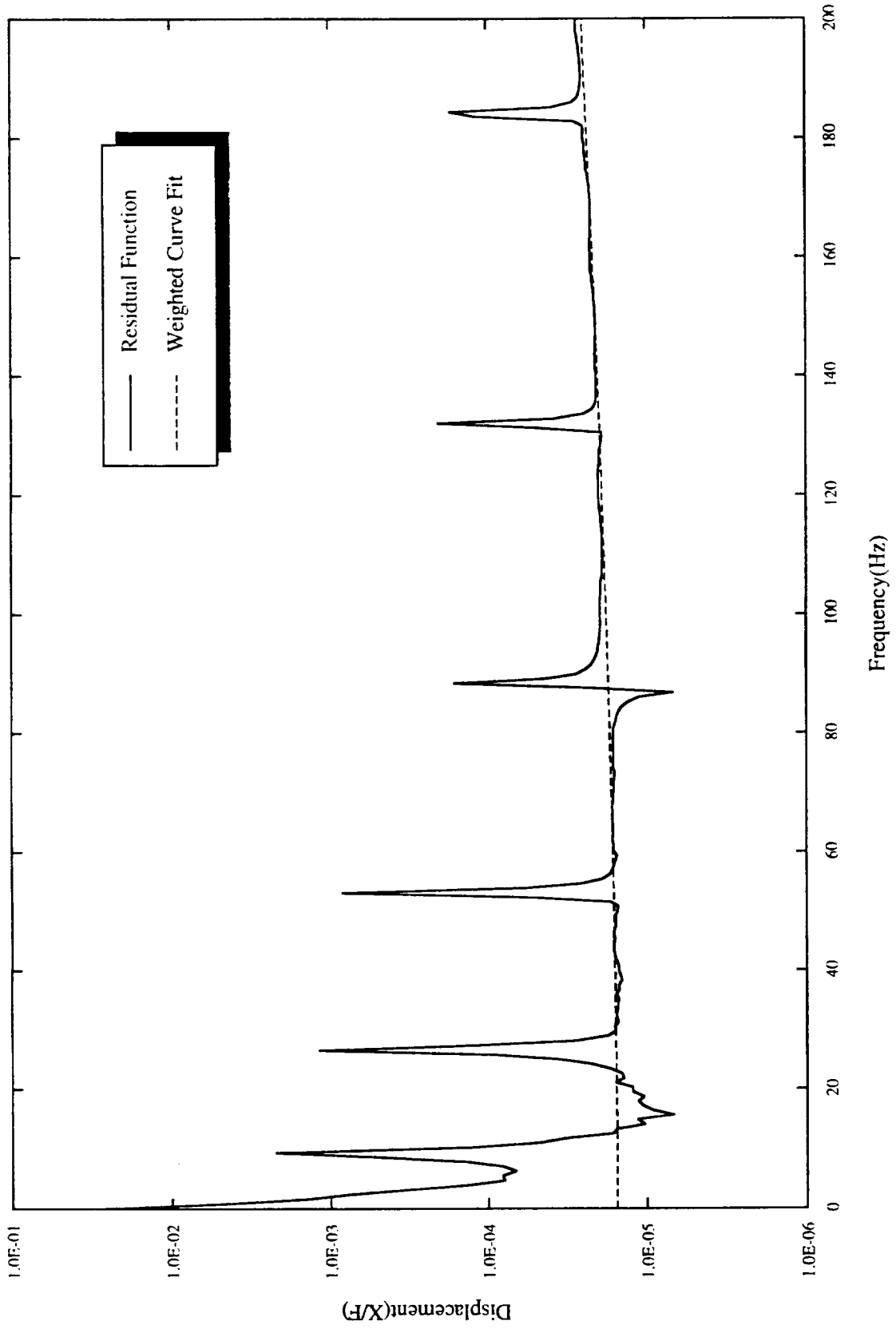


Figure 16. Weighted curve fit of residual function for beam.

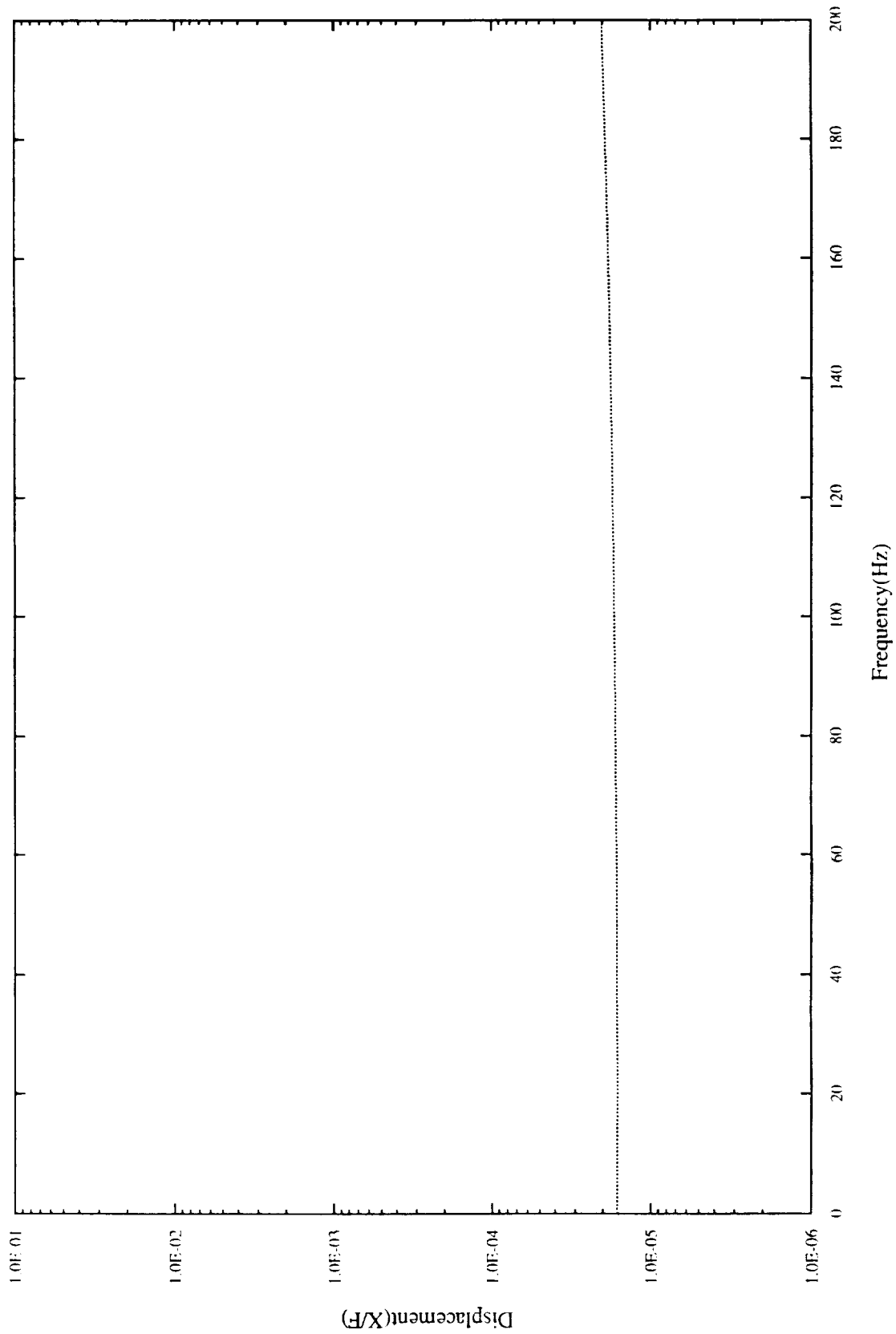


Figure 17. Theoretically generated residual function from beam model.

Table 3. Residual flexibility curve fitting errors for beam.

Lower Frequency	Upper Frequency	2 Points	Percent Error	3 Points	Percent Error	4 Points	Percent Error
Exact		1.6165e-5	0.00	1.6165e-5	0.00	1.6165e-5	0.00
0	200	1.5761e-5	2.52	1.6035e-5	0.81	1.5833e-5	2.06
30	200	1.5757e-5	2.53	1.6035e-5	0.80	1.5835e-5	2.04
60	200	1.5771e-5	2.44	1.6225e-5	0.37	1.5865e-5	1.86
0	180	1.5758e-5	2.52	1.6066e-5	0.61	1.5888e-5	1.71
30	180	1.5758e-5	2.52	1.6067e-5	0.60	1.5890e-5	1.70
60	180	1.5772e-5	2.43	1.6268e-5	0.64	1.5923e-5	1.50

variation in table 3 is insignificant. The comparison of the utilization of two, three, and four consecutive data points to generate the weighting function shows a small change with three points producing the best results.

The larger error in the two- and four-point evaluation can be attributed to the distribution of the data point of the curve. For instance, if two consecutive data points straddle a peak (define the peak) at equal heights, their variance may be low but their overall magnitude is greater than the characteristic curve. A high weighting value would be assigned that would produce an incorrect curve fit (i.e., residual flexibility value).

After the test mode shapes and natural frequencies have been obtained, the data manipulation was performed by programs written in MATLAB™ by The MathWorks. The program MK-Phi-FRF.m takes the mathematical model's mass and stiffness matrices and generates the natural frequencies, mode shapes, and appropriate drive-point FRF for the response function approach. MK-Phi-FRF.m sets up the input parameters for the program rbfcfv.m. The program rbfcfv.m, which utilizes the response function approach, computes the residual function from the drive-point FRF and generated elastic and rigid-body response functions. A weighting function is generated and applied to the curve fit of the residual function, producing the residual terms. The program res.m uses the matrix approach to generate the residual terms from a mathematical model. The programs MK-Ph-FRF.m, rbfcfv.m, and res.m can be found in the appendices. Each program is documented and has the appropriate equation reference.

VI. APPLICATION TO PALLET SIMULATOR

Once the method and programs have been verified on a simple structure (beam) with a known exact (theoretical) answer, the implementation on a more complex structure is to be performed. A frame structure (fig. 18) has been designed and built to simulate a space shuttle cargo pallet. The fundamental mode distribution and trunnion modes of the frame structure are similar to a space shuttle cargo pallet.

A theoretical "exact" solution is not available for the pallet simulator. To obtain the closest model representation to the physical structure, the mathematical model (FEM) is to be correlated to the elastic modes obtained from the modal test data. All the elastic modes up to the first bending mode of

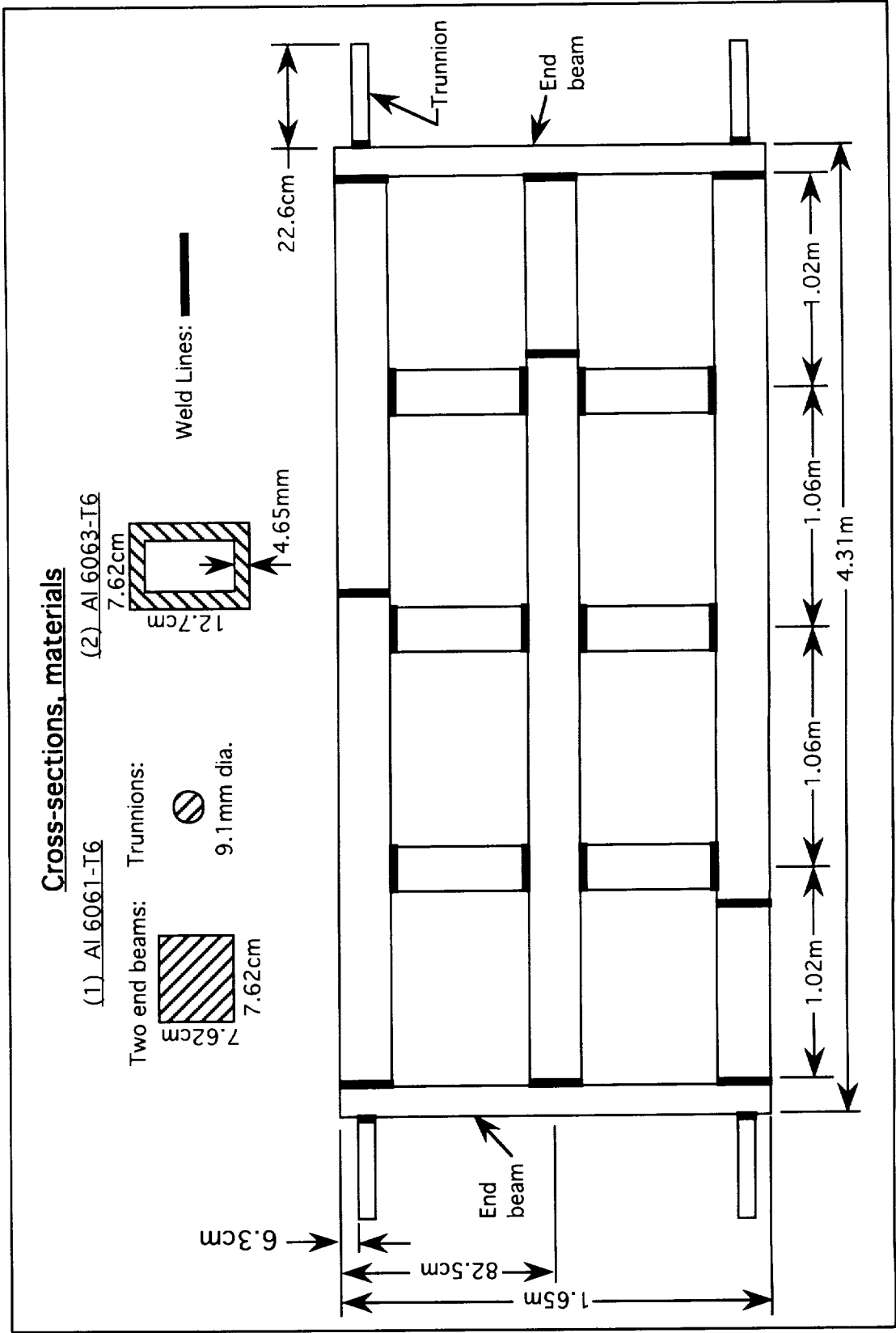


Figure 18. Space shuttle pallet simulator.

the trunnions are to be correlated. In an actual test, only a subset of the elastic modes (up to a prechosen cutoff frequency) would be used in the correlation. In this analysis, the first eight natural frequencies are used in the determination of the residual values. Since the mathematical model is correlated through the 14 elastic modes, the use of the model to predict the residual terms of the first eight modes can be accomplished with confidence.

The free-free modal test hardware setup consists of a Hewlett Packard 9000/750 workstation with a Hewlett Packard 3565S frontend for data acquisition (fig. 19). The accelerometers utilized during the modal test were PCB Piezotronics STRUCTCEL™ accelerometers. LMS software was employed, with their FMON™ package for data acquisition and the MODAL™ package for modal parameter estimation.

The pallet simulator was suspended by bungy cords in a free-free environment. The modal test was conducted using random vibration shaker excitation in the three translational directions in sequence (fig. 20). The mathematical model was then correlated to the first 14 elastic natural frequencies and mode shapes. The results of the correlation are found in table 4. With a frequency difference less than 1 percent and MAC values of 1.00, an “exact” mathematical model is said to be obtained.

The drive-point FRF's are to be measured at the points where the structure would connect (interface) with its environment (end of the trunnions). A hammer impact excitation was used to excite the structure with a data acquisition frequency range up to 100 Hz. If the shaker was attached to the end of the trunnion, mass and stiffness loading would occur due to the size of the trunnion and would impose additional uncertainties in the data. The response function at the other interface points was acquired for each drive-point excitation with a total of 144 FRF's obtained.

Examining one of the drive-point FRF's, modal parameters (mode shapes and natural frequencies) were extracted for the first eight elastic modes. Using these eight modes, a synthesized FRF was generated. The synthesized and the drive-point FRF's are plotted together (fig. 21) for visual comparison. The frequency range in figure 21 has been extended to show their relationship. Subtracting the synthesized FRF from the drive-point FRF, the residual function was generated (fig. 22). It can be seen that a direct curve fit of the residual function would cause extreme divergence as in the beam's residual function curve fit.

A weighting function was generated using three consecutive data points (fig. 23). Applying the weighted curve fit to the residual function, the residual flexibility and residual mass are found to be $7.6738e-6$ and $5.6104-12$, respectively (fig. 24). The residual terms from the “exact” mathematical model were computed and compared to the test-generated residual terms with test errors of 2.50- and 1.36-percent for flexibility and mass, respectively. The number of consecutive data points and the frequency range for weighting function generation were changed to verify the curve fitting process (table 5). Similar variation in the percent error was observed as in the beam results.

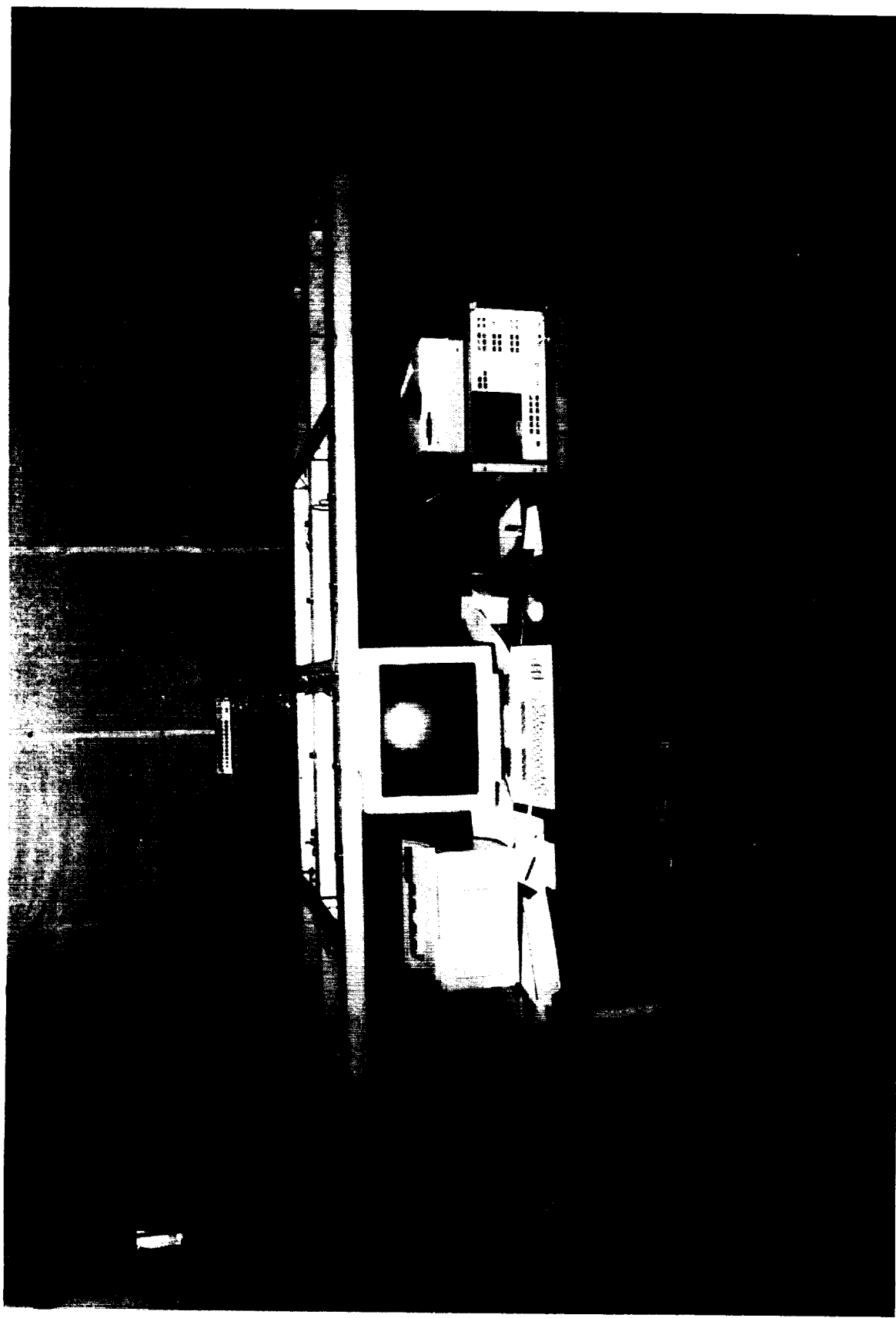


Figure 19. Modal test setup and test equipment.

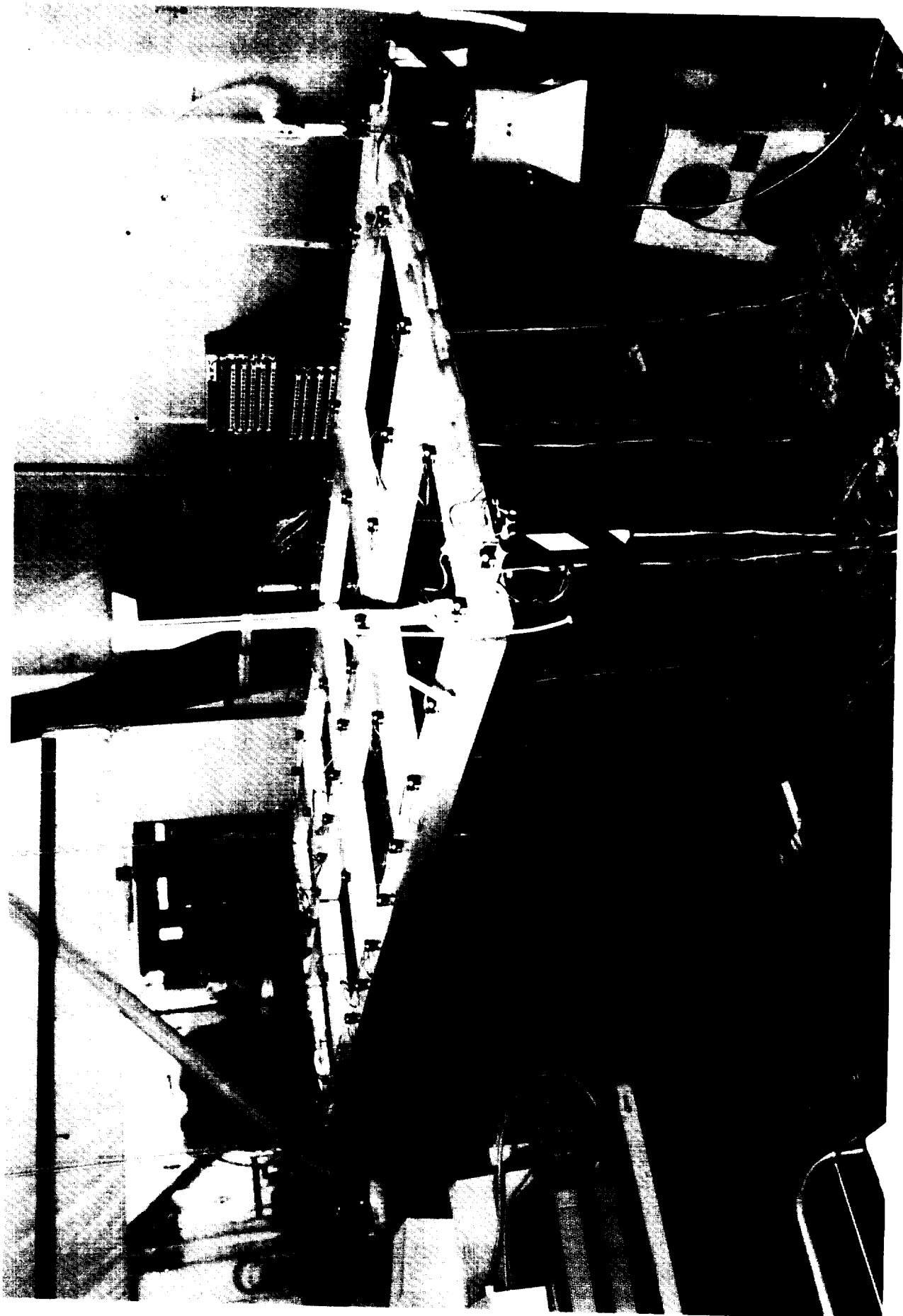


Figure 20. Free-free modal test configuration.

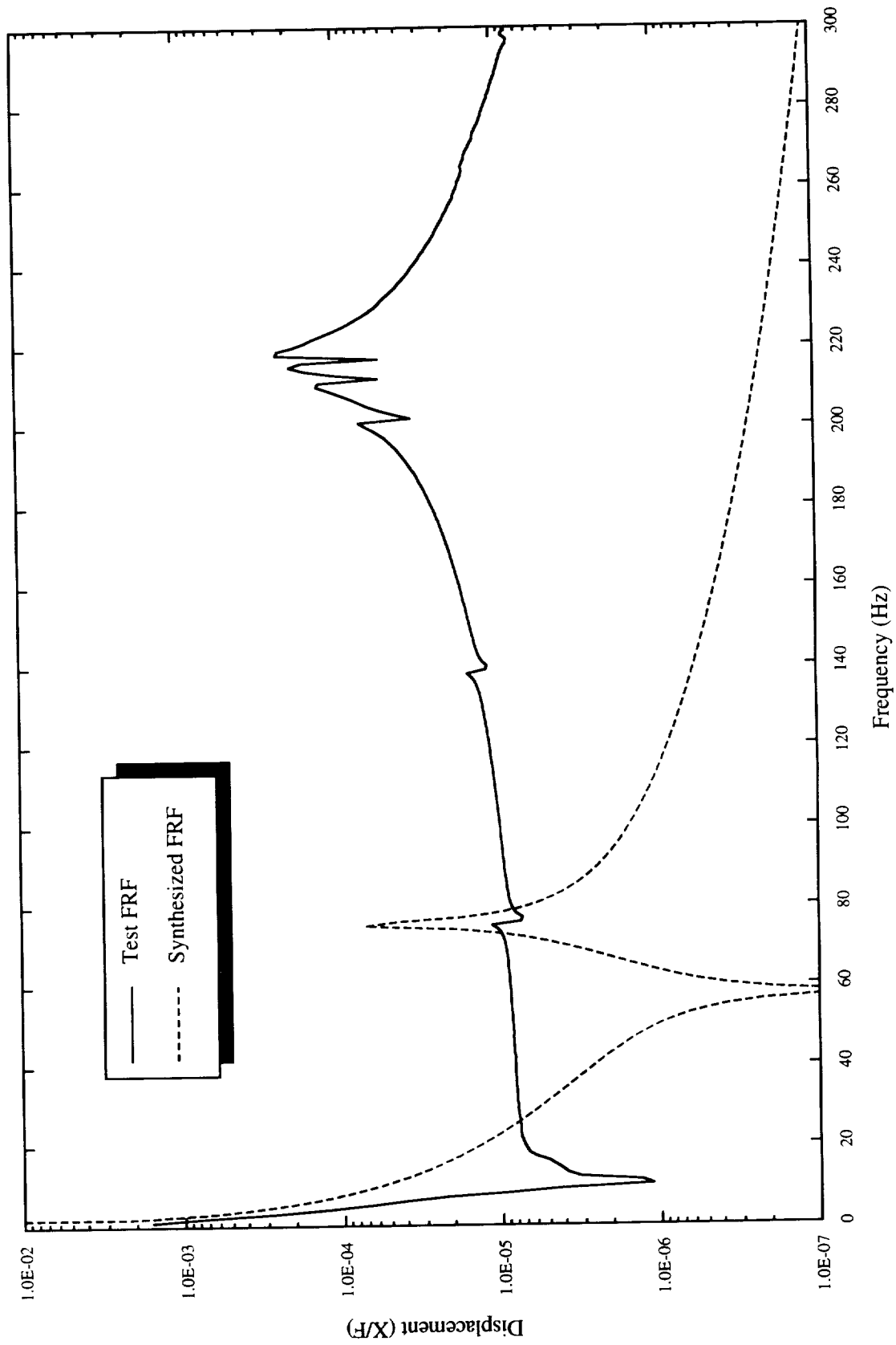


Figure 21. Overlay of test and synthesized drive-point FRF's for pallet simulator.

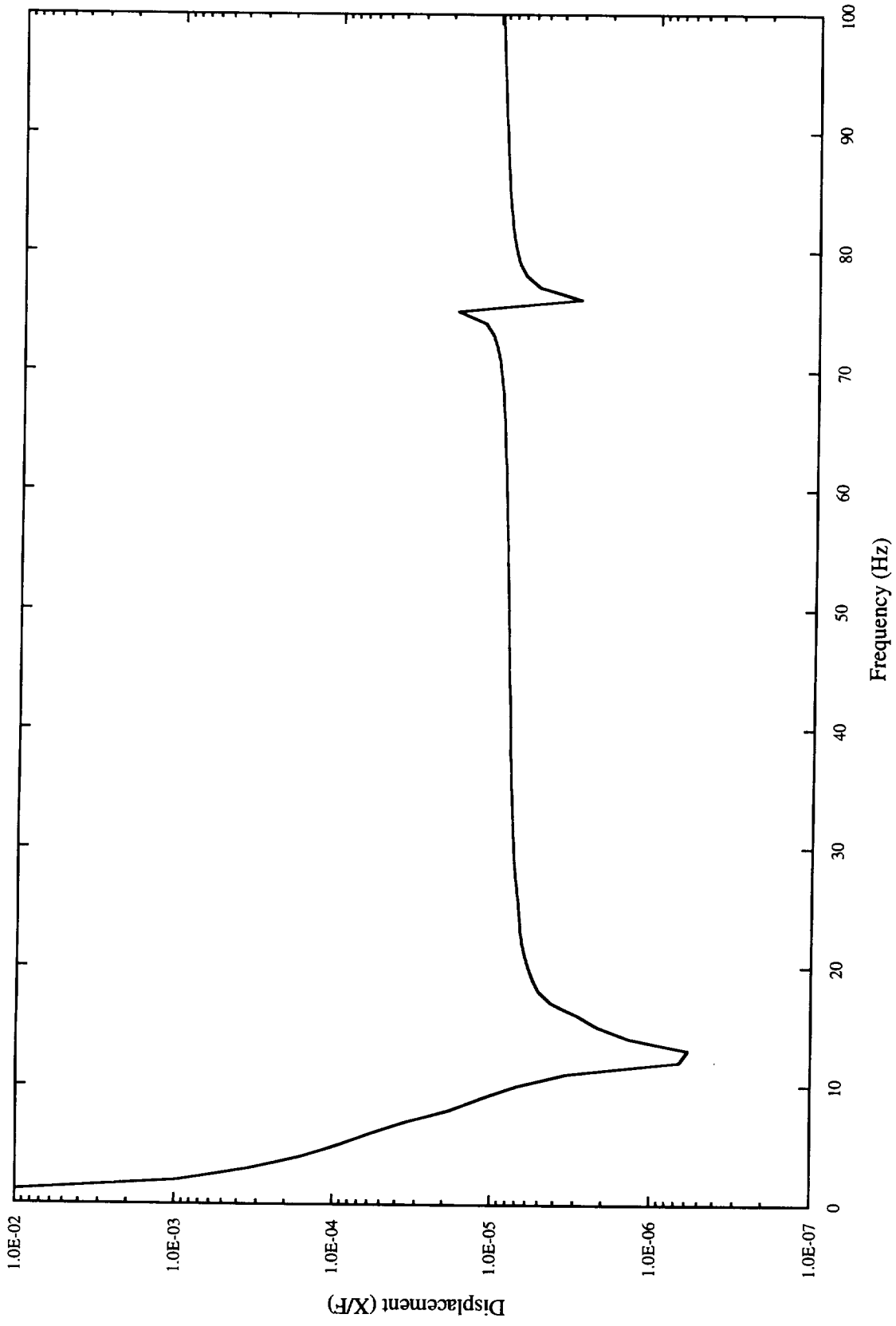


Figure 22. Residual function for pallet simulator.

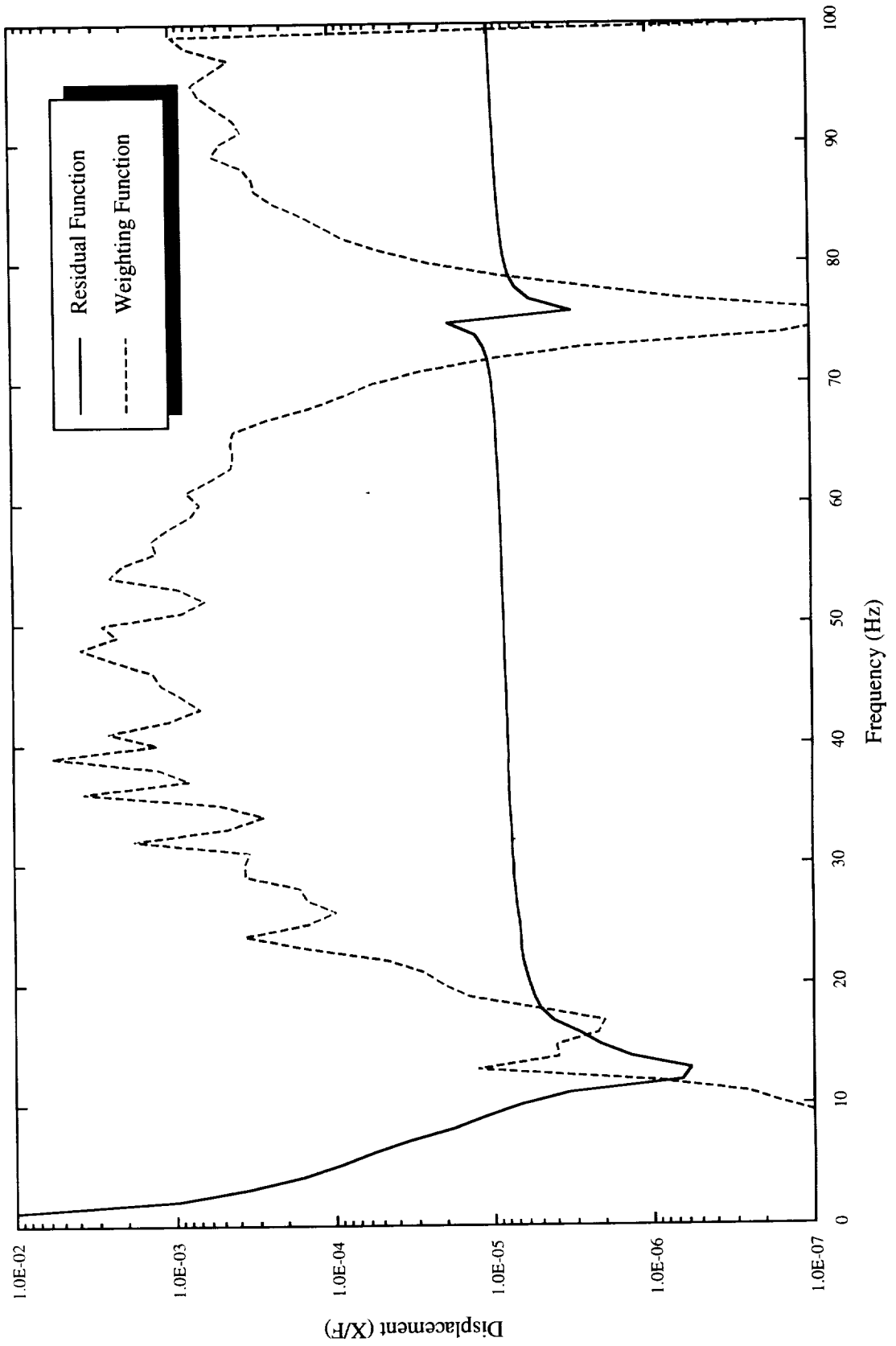


Figure 23. Weighting function for pallet simulator.

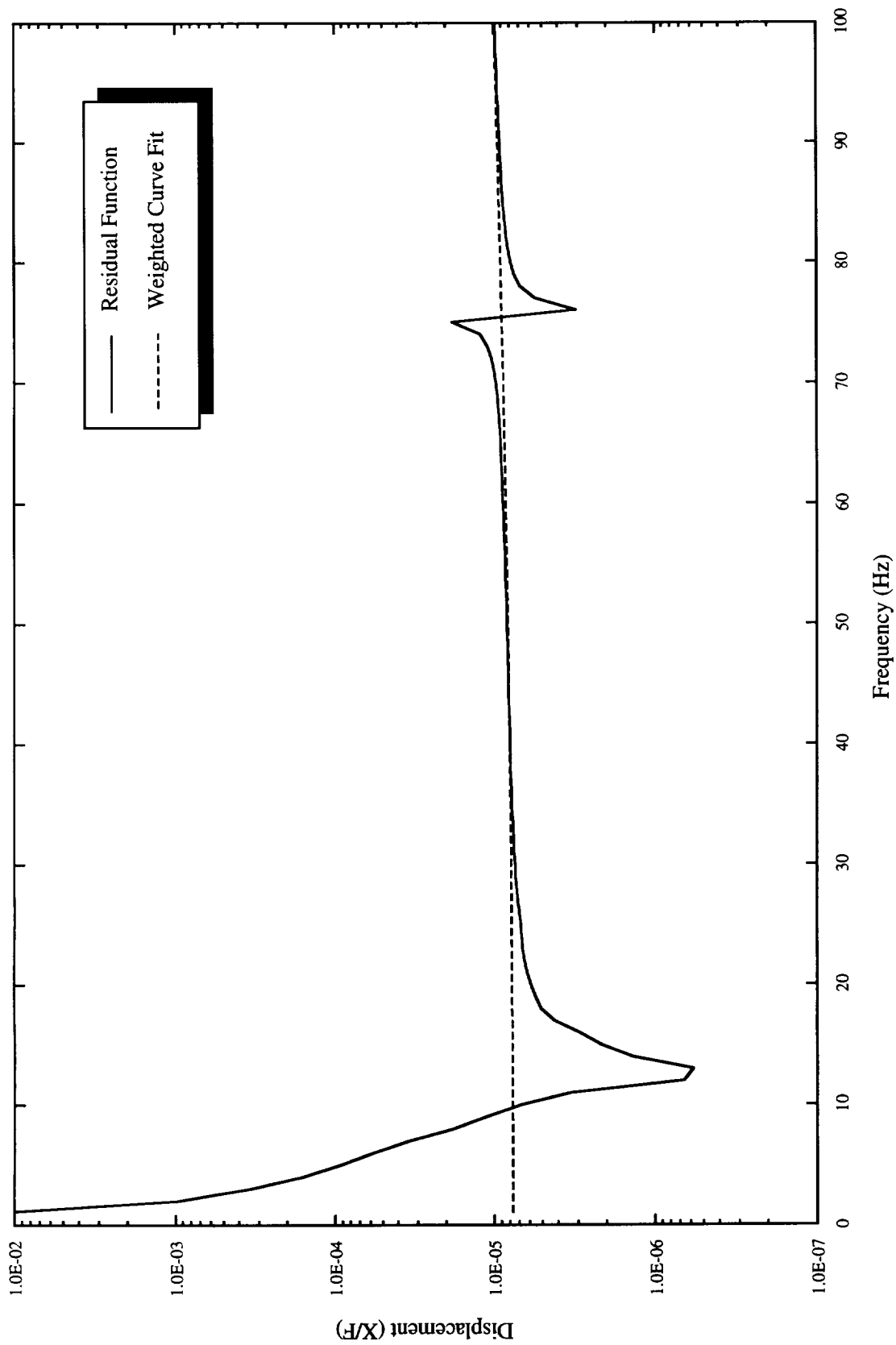


Figure 24. Weighted curve fit of residual function for pallet simulator.

Table 4. Correlation results for pallet simulator.

Mode Number	Test Frequency (Hz)	Model Frequency (Hz)	Difference (Hz)	Difference (Percent)	MAC
1	16.5620	16.5274	-0.0346	0.21	1.00
2	21.2079	21.3203	0.1124	0.53	1.00
3	46.4941	46.1600	-0.3341	0.72	1.00
4	51.3995	51.5989	0.1994	0.39	1.00
5	75.7266	75.3772	-0.3494	0.46	1.00
6	83.7987	84.4266	0.6279	0.75	1.00
7	96.7800	96.1199	-0.6601	0.68	1.00
8	98.6837	98.4312	-0.2525	0.26	1.00
9	105.7185	106.0403	0.3218	0.30	1.00
10	112.8742	113.1375	0.2633	0.23	1.00
11	135.6785	136.2627	0.5842	0.43	1.00
12	136.6981	137.9833	1.2852	0.94	1.00
13	138.6954	139.4763	0.7809	0.56	1.00
14	167.3594	167.7916	0.4322	0.26	1.00

Table 5. Curve fitting errors of pallet simulator residual flexibility.

Lower Frequency	Upper Frequency	2 Points	Percent Error	3 Points	Percent Error	4 Points	Percent Error
Exact		7.8707e-6		7.8707e-6		7.8707e-6	
0	100	7.5776e-6	3.72	7.6738e-6	2.50	7.6923e-6	2.27
20	100	7.6056e-6	3.37	7.6842e-6	2.37	7.7037e-6	2.12
40	100	7.8214e-6	0.63	7.9305e-6	0.76	7.9457e-6	0.95
0	90	7.2536e-6	7.84	7.5488e-6	4.09	7.5553e-6	4.01
20	90	7.3175e-6	7.03	7.5658e-6	3.87	7.5764e-6	3.74
40	90	7.7639e-6	1.36	7.9176e-6	0.60	7.9368e-6	0.84

VII. CONCLUSION

An applicable least-squares curve fitting procedure using a statistically generated weighting function has been developed. This curve fitting procedure enables the accurate curve fitting of test-generated residual functions that contain regions of ragged data. The ragged data is the result of the inability to accurately evaluate the modal parameters from the FRF during the modal testing process. Programs for calculating the residual terms from modal test data and a mathematical model (FEM) have been written in MATLAB™. The curve fit of the drive-point residual function for a beam with a trunnion type interface, retaining the first six elastic modes, produced residual flexibility values with errors in the 0.4- to 2.5-percent range. The errors were determined by comparing the residual terms of the test data to the residual terms generated from a mathematical model which was correlated to the exact theoretical solution.

The curve fitting process was also applied to a frame structure that simulates a space shuttle cargo pallet, which is more complex than a straight beam. The residual flexibility values for the pallet simulator, retaining the first eight elastic modes, were found to be in the 0.6- to 4.0-percent range. A theoretical solution is not available for the frame structure. The “exact” answer was generated by correlating the mathematical model to all the elastic natural frequencies and mode shapes up to the first bending mode of the trunnion (i.e., 14 elastic modes).

The development of the weighted curve fit of the residual function has made possible further investigation of the residual flexibility modal testing technique. Additional studies are needed in the area of modal parameter estimation, since this is the cause of the ragged data in the residual function. The next step, which is also under investigation, is how to use the residual flexibility to accurately correlate a mathematical model.

REFERENCES

1. Admire, J.R., Ivey, E.W., and Tinker, M.L.: "Mass-Additive Modal Test Method for Verification of Constrained Structural Models." Proceedings of the 10th International Modal Analysis Conference, February 1992.
2. Coleman, A.D.: "A Mass Additive Technique for Modal Testing as Applied to the Space Shuttle ASTRO-1 Payload." Proceedings of the Sixth International Modal Analysis Conference, February 1988, pp. 154–159.
3. Barney, P.S.: "Investigation of Mass Additive Testing for Experimental Modal Analysis." Dissertation at the University of Cincinnati, 1992.
4. Rubin, S.: "Improved Component Mode Representation for Structural Dynamic Analysis." AIAA Journal, vol. 13, 1975, pp. 995–1006.
5. MacNeal, R.H.: "A Hybrid Method of Component Mode Synthesis." Computers and Structures, vol. 1, 1971, pp. 581–601.
6. Martinez, D.R., Carne, T.G., and Miller, A.K.: "Combined Experimental/Analytical Modeling Using Component Mode Synthesis." Proceedings of the 25th Structures, Structural Dynamics, and Materials Conference, 1984, pp. 140–152.
7. Admire, J.R., Tinker, M.L., and Ivey, E.W.: "Residual Flexibility Test Method for Verification of Constrained Structural Models." Proceedings of the 33rd Structures, Structural Dynamics, and Materials Conference, 1992, pp. 1614–1622.
8. Klosterman, A.L., and Lemon, J.R.: "Dynamic Design Analysis Via the Building Block Approach." Shock and Vibration Bulletin, No. 42, part 1, 1972, pp. 97–104.
9. Flanigan, C.C.: "Test-Analysis Correlation of the Transfer Orbit Stage Modal Survey." Report 40864-8 SDRC, Inc., San Diego, CA, October 1988.
10. Blair, M.A.: "Space Station Module Prototype Test Report: Free-Free Testing Methods." Lockheed Missiles and Space Company, Sunnyvale, CA, EM ATTIC 001, June 1991.
11. Smith, K., and Peng, C.Y.: "SIR-C Antenna Mechanical System Modal Test and Model Correlation Report." Jet Propulsion Laboratory, Pasadena, CA, JPL D-10694, vol. 1, April 1993.
12. Craig, R.R., and Bampton, M.C.C.: "Coupling of Substructures for Dynamic Analyses," AIAA Journal, vol. 6, No. 7, 1968, pp. 1313–1319.
13. Miller, I.R., Freund, J.E., and Johnson, R.: "Probability and Statistics for Engineers." Prentice Hall, NJ, 1990, pp. 22–30.
14. Blevins, R.D.: "Formulas for Natural Frequency and Mode Shape." Van Nostrand Reinhold Company, NY, 1979, p. 108.

APPENDIX A

PROGRAM MK-Phi-FRF.m

The program MK-Phi-FRF.m takes the mathematical model's mass and stiffness matrices and generates the natural frequencies, modes shapes, and the appropriate drive-point frequency response function for the response function approach. MK-Phi-FRF.m sets up the input parameters for the program rbfcfv.m for the mathematical model data. The input parameters are set up to run the beam problem.

```
% PROGRAM MK-Phi-FRF.m
%
% This program computes from the Mass and Stiffness matrices
% of a FEM program, the eigenvalues and eigenvectors. It then
% computes the Frequency Responce Function for a specified
% responce point and excitation point. The frequencies and
% mode shapes are split up into rigid body and elastic
% components.
%
% Note: The mass & stiff. matrices must be stored in matlab
%       format with the matrices names as "M" & "K"
%       respectively.
clear
echo off
prename=input('Enter PreName? ','s');

% Set Flag for following generating FRF corresponding to
% 0-Full, 1-Elastic, 2-Rigid Body, 3-No FRF
Flag=0;

j=26;           % drive coordinate
k=26;           % responce coordinate
nrbm=6;         % number of rigid body modes
nrem=6;         % number of elastic modes
xdofs=[27];     % DOF to exclude from analysis
StFreq=0.0;     % start frequency in Hz.
step=0.78125;   % delta-f, frequency step in Hz.
dim=512;        % size of frf to be generated

eval(['load ',prename, '.MK.mat']);
[m,m]=size(M);
FRF=zeros(1,dim)';
```

```

f=linspace(StFreq,dim*step,dim)';
f=f(1:dim);
Rad=f*(2*pi);

% compute mode shape and frequencies
disp(' Computing Eigenvalues and Eigenvectors')
[Phi,w,Freq,GM]=EignSol2(M,K);

% separate elastic and rigid body modes
disp(' Separate Elastic and Rigid Body Modes')
Phi(xdofs,:)=[];
Phie=Phi(:,nrbm+1:nrbm+nrem);
Phirb=Phi(:,1:nrbm);
Freqe=Freq(nrbm+1:nrbm+nrem);
Freqrb=Freq(1:nrbm);

% save modal parameters
eval(['save ',[prename,'.Elas.mat'],' Freqe Phie']);
eval(['save ',[prename,'.RB.mat'],' Freqrb Phirb']);

% Generate Full FRF
if Flag==0
disp(' Processing Full FRF')
Lambda=zeros(dim,m-1);
Phi2=Phi(j,:).*Phi(k,:);
Rad2=Rad.^2;
r=1;
while r<=m-1
FRF=FRF+(Phi2(r)./(Freq(r)^2-Rad2));
r=r+1;
end
end

% Generate Elastic FRF
if Flag==1
disp(' Processing Elastic FRF')
Lambda=zeros(dim,nrem);
Phi2=Phie(j,:).*Phie(k,:);
i=1;
r=1;
while r<=nrem
while i<=dim;
Lambda(i,r)=(Phi2(r)/(Freqe(r)^2-Rad(i)^2));
i=i+1;
end
i=1;
FRF(:)=FRF(:)+Lambda(:,r);
r=r+1;
end
end

% Generate Rigid Body FRF
if Flag==2

```

```

disp(' Processing Rigid Body FRF')
xf=zeros(dim,nrbm);
Phi2=Phirb(j,:).*Phirb(k,:);
i=1;
r=1;
while r<=nrbm
    while i<=dim;
        Lambda(i,r)=(Phi2(r)/(Freqrb(r)^2-Rad(i)^2));
        i=i+1;
    end
    i=1;
    FRF(:)=FRF(:)+Lambda(:,r);
    r=r+1;
end
end

% save FRF in (displacement/f) format
eval(['save ',[prename,'.',int2str(j)],'.',int2str(k),
        '.FRF.mat'],' FRF');
disp(' FRF Saved in x/f format')

% plot FRF
semilogy(f,abs(FRF))
title(['Filename ',prename,': Drive',num2str(j), ...
        ' - Response',num2str(k)])
xlabel('Freq')
ylabel('X/F')

% DESCRIPTION OF TERMS
% j          drive point DOF
% k          response point DOF
% nrbm       number of rigid body modes
% nrem       number of elastic modes
% xdofs      DOFS to exclude from the analysis
% StFreq     frequency for the FRF to start
% step       frequency step (resolution) in Hz.
% dim        dimension of the FRF (size)
% FRF        vector containing the FRF
% f          frequency values in Hz.
% rad        frequency values in radians
% M          mass matrix
% K          stiffness matrix
% Phi        eigenvectors
% Freq       eigenvalues in radians
% w          eigenvalues in radians on main diagonal
% GM         generalized mass
% Phie,Phirb elastic and rigid body eigenvectors
% Freqe,Freqrb elastic and rigid body eigenvalues

```


APPENDIX B

PROGRAM rbf.m

The program rbf.m, which utilizes the response function approach, computes the residual function from the drive-point FRF and generated elastic and rigid-body response functions. A weighting function is generated and applied to the curve fit of the residual function producing the residual terms. The input parameters are set up to run the beam problem.

```

% PROGRAM rbf.m
%
% Computes the Residual Function and performs a weighted least
% square curve fit of the Residual Function.
  clear
  echo off
  i=sqrt(-1);

% Required input
  j=26;           % drive point DOF
  k=26;           % response point DOF
  HzStep=0.78125; % squared resolution (Delta Hz)
  n=512;          % number of data points
  HzStFreq=0.78125; % start frequency in Hertz
  dptl=100;       % lower data pt to consider in curve fit
  dptu=256;       % upper data pt to consider in curve fit
                  % dptl & dptu for flexibility of range
                  % in curve fit
  num'sample=3;   % # of data samples to use in forming weighting
                  % function (range 2-6).Note: if 5 or 6 change
                  % w(r+1,r+1)= to w(r+2,r+2)=

% Load Data from MATLAB Format Files
% prename.Elas.mat contains Free-Free Frequencies and Modes
%   ("Frege, Phie")
% prename.FRF.mat contains Test FRF("FRF")
% prename.RB.mat contains Rigid Body Frequencies and Modes
%   ("Fregrb, Phirb")
  prename=input('Enter PreName? ','s');
  eval(['load ',prename, '.Elas.mat']);
  eval(['load ',prename, '.FRF.mat']);
  eval(['load ',prename, '.RB.mat']);

```

```

% Setup Parameters and Initialize Matrices
    [tmp,nrem]=size(Phie);
    [tmp,nrbm]=size(Phirb);
    Hz=linspace(HzStFreq,n*HzStep,n)';
    Hz=Hz(1:n);
    RadSqd=(Hz.*(2*pi)).^2;
    FRF=FRF(2:n+1);
    FRFe=zeros(1,n)';
    FRFrb=zeros(1,n)';
    w=zeros(n,n);
    xx=zeros(2,1);

% Synthesize Elastic Mode FRF, from Equ. 3.2
disp(' Synthesize Elastic Mode FRF')
Phie2=Phie(j,:).*Phie(k,:);
    r=1;
    while r<=nrem
        FRFe=FRFe+(Phie2(r)./(Frege(r)^2.-RadSqd));
        r=r+1;
    end

% Generate Rigid Body FRF, from Equ. 3.2
disp(' Generate Rigid Body FRF')
Phirb2=Phirb(j,:).*Phirb(k,:);
    r=1;
    while r<=nrbm
        FRFrb=FRFrb+(Phirb2(r)./(Fregrb(r)^2.-RadSqd));
        r=r+1;
    end

% Subtract Ridged Body and Elastic FRFs from Test FRF,
% from Equ. 3.2
retFRF=(FRFrb)+(FRFe);
ResFRF=((FRF)+(retFRF));

% Computing Weighting Function, Equ. 4.1
disp(' Computing Weighting Function')
b=abs(ResFRF);
    r=dptl;
    while r<=dptu-(num'sample-1)
        w(r+1,r+1)=1/(std(b(r:r+(num'sample-1))))^2;
        if w(r+1,r+1) == Inf
            disp(' *** Variance = 0.0 Substituting 1.0e+10 ***')
            w(r+1,r+1)=1.0e+10; %value may need to be changed to fit mean
        end
        r=r+1;
    end

% Normalize Weighting Function
w=w./max(max(w));

% Forming "A" matrix, from Equ. 3.8

```

```

A=RadSqd;
A(:,2)=ones(n,1);

% Solving for Unknowns, from Equ. 4.3
disp(' Solving for Unknowns')
xx=(A'*w*A)\(A'*w*b);
Gr=xx(2,1);
Hr=xx(1,1);

% Computing Curve Fit, from Equ. 3.8
disp(' Computing Curve Fit')
cfit=A*xx;

% Saving Residual Terms and FRF
eval(['save ',[prename,'.Res.mat'],' Gr Hr ResFRF']);

% Plot Residual FRFs
semilogy(Hz,abs(ResFRF),'r-',Hz,abs(retFRF),'g-',...
          Hz,abs(FRF),'w:');
title('Frequency Response Functions for Residual Flexibility')
xlabel('Frequency (Hz)')
ylabel('Displacement (x/f)')
legend('Residual Function','Synthesized','Measured');

%print
disp('      ** Screen is PAUSED. Enter or Return to continue **')
pause

% Plot Curve Fit ant Etc.
semilogy(Hz,abs(b),Hz,abs(cfit),Hz,abs(diag(w)))
title('Difference FRF & Curve Fit')
xlabel('Frequency (Hz)')
ylabel('Displacement (x/f)')
legend('Residual Function','Curve Fit','Weighting Function');

ResTerms=...
sprintf('\n Residual Terms\n  Gr = %10.8e\n  Hr = %10.8e',Gr,Hr);
disp(ResTerms);

% DESCRIPTION OF TERMS
% A          matrix of coefficients of the unknowns
% cfit       curve fit of residual function
% FRF        test frequency response function
% FRFe       synthesized FRF from elastic modes
% FRFr       synthesized FRF from rigid coefficient modes
% Gr,Hr      residual flexibility and residual mass
% Hz         vector of frequencies in hertz for plotting
% nrem       number of retained elastic modes
% nrbr       number of rigid body modes
% Phie, Frege elastic modal properties
% Phie2      the square of each term in Phie
% Phirb, Freqrb rigid body modal properties
% Phird2     the square of each term in Phirb
% RadSqd     vector of frequencies in radians, terms squared

```

```
% ResFRF      residual function
% retFRF      synthesized FRF of retained modal parameters
% w           matrix with weighting function on main diagonal
% xx          contains residual mass and flexibility
```


APPENDIX C

PROGRAM res.m

The program res.m uses Rubin's matrix approach to generate the residual terms from a mathematical model. This program also computes the constrained natural frequencies and mode shapes from a subset of free-free modes and drive-point residual flexibilities.⁷ The input parameters are set up to run the beam problem.

```
% PROGRAM res.m
%
% This program computes the residuals and the constrained mode
% shapes generated from the residual flexibility.
% See discription of terms at end of program.
clear
echo off
% input data
prename=input('Enter PreName? ','s');
iDof=[26];
ConDof=[26];
rm=[1 2 3 4 5 6 7 8];
nrbm=2;
eval(['load ',prename,'.MK.mat']);

% reorder M&K so interface DOF's are in last Rows & Columns,
% generate mode Shapes
disp(' Calculating eigenvalues and eigenvectors')
niDof=length(iDof);
nConDof=length(ConDof);
nrm=length(rm);
[n,n]=size(M);
o1=[1:n];
o1(iDof)=[];
o1(n-niDof+1:n)=iDof;
M=M(o1,o1);
K=K(o1,o1);
[Phi,w,Freq,GM]=EignSol2(M,K);

% construct transformation from constrained to free-free
% assumes rigid body modes are in first columns, from Equ. 2.8
Phirb=Phi(:,1:nrbm);
A=eye(n)-M*Phirb*Phirb';
```

```

% generate constrained stiffness, constrained flexibility, and
% free-free flexibility matrix, from Equ. 2.12
disp(' Generating flexibility matrices')
Kc=K;
StConDof=n-nConDof+1;
Kc(StConDof:n,StConDof:n)=Kc(StConDof:n,StConDof:n)+...
diag(diag(Kc(StConDof:n,StConDof:n)));
Gc=inv(Kc);
G=A'*Gc*A;

% generate retained flexibility matrix and
% remove from full flexibility matrix, from Equ. 2.15
disp(' Generate Retained Flexibility Matrix')
Kn=w(rm,rm).^2;
Kn=Kn(nrbm+1:nrm,nrbm+1:nrm);
Phin=Phi(:,rm);
Phin=Phin(:,nrbm+1:nrm);
Gn=(Phin/Kn)*Phin';
Gr=G-Gn;

% partition mode shapes and retained flexibility
disp(' Partition Matrices')
Phiki=Phi(1:n-niDof,rm);
Phikb=Phi(n-niDof+1:n,rm);
Grib=Gr(1:n-niDof,n-niDof+1:n);
Grbb=Gr(n-niDof+1:n,n-niDof+1:n);

% generate full residual mass and extract boundary mass terms,
% from Equ. 2.17
Hr=Gr'*M*Gr;
Hrbb=Hr(n-niDof+1:n,n-niDof+1:n);

% THE FOLLOWING IS AN IMPLEMENTATION OF THE PROCEDURE FOUND
% IN REFERENCE [7].

% generate transformation matrix
disp(' Generate Transformation Matrix')
tmp=Grib/Grbb;
[tmpm,tmpn]=size(tmp);
T=Phiki-tmp*Phikb;
[tm,tn]=size(T);
T(1:tm,tn+1:tn+tmpn)=tmp;
T(tm+1:n,1:tn)=zeros(n-tm,tn);
T(tm+1:n,tn+1:tn+tmpn)=eye(n-tmpm,tmpn);

% form constrained model, solve, and convert solution to
% physical coordinates
disp(' Form Constrained Model, Solve, and')
disp(' Convert to Physical Coord.')
Mb=T'*M*T;
Kb=T'*K*T;
Mnn=Mb(1:nrm,1:nrm);
Knn=Kb(1:nrm,1:nrm);

```

```

[Phinn,wc]=EignSol(Mnn,Knn);
Phinn(nrm+1:nrm+tmpn,1:nrm)=zeros(tmpn,nrm);
Phic=T*Phinn;

% exact solution by FEM
disp(' Exact Solution by FEM')
Ke=K(1:n-nConDof,1:n-nConDof);
Me=M(1:n-nConDof,1:n-nConDof);
[Phie,we,Frege,GMe]=EignSol2(Me,Ke);
Phie(n-nConDof+1:n,1:n-nConDof)=zeros(nConDof,n-nConDof);

% checking orthogonality
Orthog= Phie'*M*Phic;

% saving data
eval(['save ',[prename,'.res.mat'],' Grbb Hrbb Orthog..
/ascii']);
disp(' That's All Folks')

% DESCRIPTION OF TERMS
% niDof      number of interface DOFs.
% iDof       row or column corresponding to the interface DOF.
% nConDof    number of constrained DOF for determinatly
%            constrained model.
% ConDof     constrained DOF for determinatly constrained model
% nrm        number of retained modes.
% rm         mode number of retained modes including r-b mode.
% nrbm       number rigid body modes.
% M,K        mass and stiffness of full model
% ol         reorder to place interface DOF's in last col & rows
% Phi        full mode shapes
% w          frequency in matrix form of full model
% Phirb      rigid body mode shapes
% A          transformation matrix for constrained flexibility
%            matrix to free-free flexibility matrix
% Kc         constrained stiffness matrix
% Gc         constrained flexibility matrix
% G          free-free flexibility matrix
% Kn, Gn     retained stiffness and flex. matrices
% Gr         residual flexibility matrix
% Phiki, Phikb retained modes, interior and boundary DOF's
% Grib, Grbb subset of Gr, interior and boundary DOF's
% T          transformation to reduce structures coordinates
% Mb, Kb     reduced mass and stiffness matrices
% Mnn, Knn   subsets of Mb and Kb respect. obtained by setting
%            boundary displacements equal to zero.
% Phinn      constrained mode shapes in reduced coordinates
% wc         freq. in matrix form of constrained model
% Phic       constrained mode shapes in full coordinates
% Me, Ke     mass and stiffness matrices for exact solution of
%            constrained model
% Phie       exact constrained mode shapes
% we         exact freq. in matrix form for constrained model
% Orthog     orthogonality of exact and constrained mode shapes

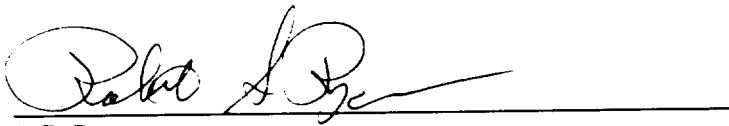
```

APPROVAL

**STATISTICALLY GENERATED WEIGHTED CURVE FIT OF RESIDUAL FUNCTIONS
FOR MODAL ANALYSIS OF STRUCTURES**

By P.S. Bookout

The information in this report has been reviewed for technical content. Review of any information concerning Department of Defense or nuclear energy activities or programs has been made by the MSFC Security Classification Officer. This report, in its entirety, has been determined to be unclassified.

A handwritten signature in black ink, appearing to read "J.C. Blair", is written over a horizontal line.

J.C. BLAIR
Director, Structures and Dynamics Laboratory

REPORT DOCUMENTATION PAGE			Form Approved OMB No. 0704-0188	
Public reporting burden for this collection of information is estimated to average 1 hour per response, including the time for reviewing instructions, searching existing data sources, gathering and maintaining the data needed, and completing and reviewing the collection of information. Send comments regarding this burden estimate or any other aspect of this collection of information, including suggestions for reducing this burden, to Washington Headquarters Services, Directorate for Information Operations and Reports, 1215 Jefferson Davis Highway, Suite 1204, Arlington, VA 22202-4302, and to the Office of Management and Budget, Paperwork Reduction Project (0704-0188), Washington, DC 20503.				
1. AGENCY USE ONLY (Leave blank)	2. REPORT DATE February 1995	3. REPORT TYPE AND DATES COVERED Technical Memorandum		
4. TITLE AND SUBTITLE Statistically Generated Weighted Curve Fit of Residual Functions for Modal Analysis of Structures			5. FUNDING NUMBERS	
6. AUTHOR(S) P.S. Bookout				
7. PERFORMING ORGANIZATION NAME(S) AND ADDRESS(ES) George C. Marshall Space Flight Center Marshall Space Flight Center, Alabama 35812			8. PERFORMING ORGANIZATION REPORT NUMBER	
9. SPONSORING/MONITORING AGENCY NAME(S) AND ADDRESS(ES) National Aeronautics and Space Administration Washington, DC 20546			10. SPONSORING/MONITORING AGENCY REPORT NUMBER NASA TM-108481	
11. SUPPLEMENTARY NOTES Prepared by Structures and Dynamics Laboratory, Science and Engineering Directorate.				
12a. DISTRIBUTION / AVAILABILITY STATEMENT Unclassified—Unlimited			12b. DISTRIBUTION CODE	
13. ABSTRACT (Maximum 200 words) <p>A statistically generated weighting function for a second-order polynomial curve fit of residual functions has been developed. The residual flexibility test method, from which a residual function is generated, is a procedure for modal testing large structures in an external constraint-free environment to measure the effects of higher order modes and interface stiffness. This test method is applicable to structures with distinct degree-of-freedom interfaces to other system components. A theoretical residual function in the displacement/force domain has the characteristics of a relatively flat line in the lower frequencies and a slight upward curvature in the higher frequency range. In the test residual function, the above-mentioned characteristics can be seen in the data, but due to the present limitations in the modal parameter evaluation (natural frequencies and mode shapes) of test data, the residual function has regions of ragged data. A second-order polynomial curve fit is required to obtain the residual flexibility term. A weighting function of the data is generated by examining the variances between neighboring data points. From a weighted second-order polynomial curve fit, an accurate residual flexibility value can be obtained. The residual flexibility value and free-free modes from testing are used to improve a mathematical model of the structure. The residual flexibility modal test method is applied to a straight beam with a trunnion appendage and a space shuttle payload pallet simulator.</p>				
14. SUBJECT TERMS residual flexibility, alternative fixed-base modal test, weight curve fit			15. NUMBER OF PAGES 61	
			16. PRICE CODE NTIS	
17. SECURITY CLASSIFICATION OF REPORT Unclassified	18. SECURITY CLASSIFICATION OF THIS PAGE Unclassified	19. SECURITY CLASSIFICATION OF ABSTRACT Unclassified	20. LIMITATION OF ABSTRACT Unlimited	

